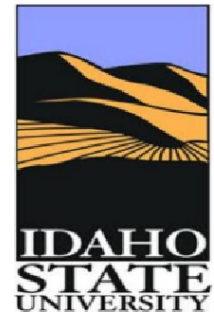
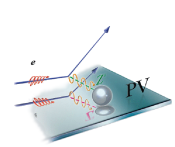


Detectors for High Flux Parity Experiments at JLab: PREX-II, CREX and MOLLER

Dustin McNulty
Idaho State University
mcnudust@isu.edu

February 3, 2020

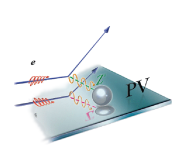




Detectors for Parity Experiments at JLab

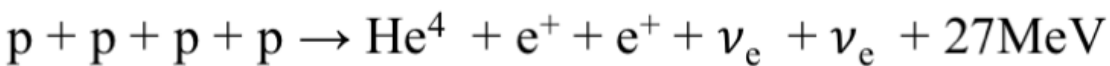
Outline

- The Weak force and Parity Symmetry Violation
- Introduction to Parity-Violating Electron Scattering
 - Why PVES?
 - Experiment blueprint, "how-to", and technical progress
- PREX-II/CREX at Jefferson Laboratory
 - Experimental concept, techniques and apparatus
- New Integrating Detectors for PV
 - PREX-I Main and A_T Detectors
 - PREX-II/CREX Main and A_T Detectors
 - Shower-max Sampling Calorimeter for MOLLER (if time)
- Summary and Future Plans



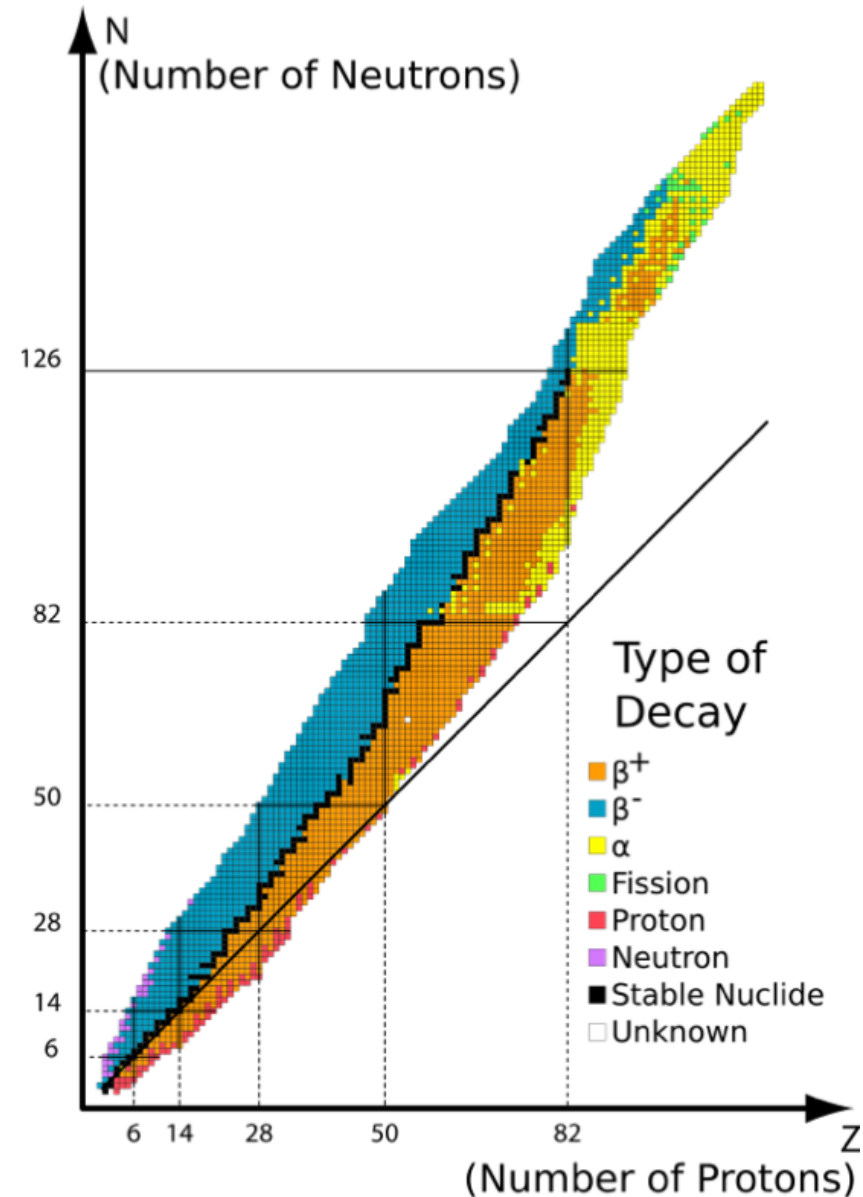
The Weak Force: Oh, I didn't know that?

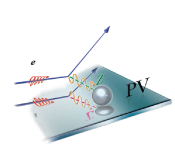
- Through a series of nuclear reactions, four protons (hydrogen nuclei) in the core of our Sun combine to form a helium nucleus emitting two positrons and two neutrinos and releasing 27 MeV of energy:



- Thermonuclear fusion--Perhaps the most important reaction for all life on planet Earth is caused by a fundamental force of nature that is rarely discussed in the classroom: Weak Interactions or the weak nuclear force

- Responsible for nearly all radioactive decay processes
- Beta decay is most common
- Theoretical understanding is at same level as Quantum Electro Dynamics

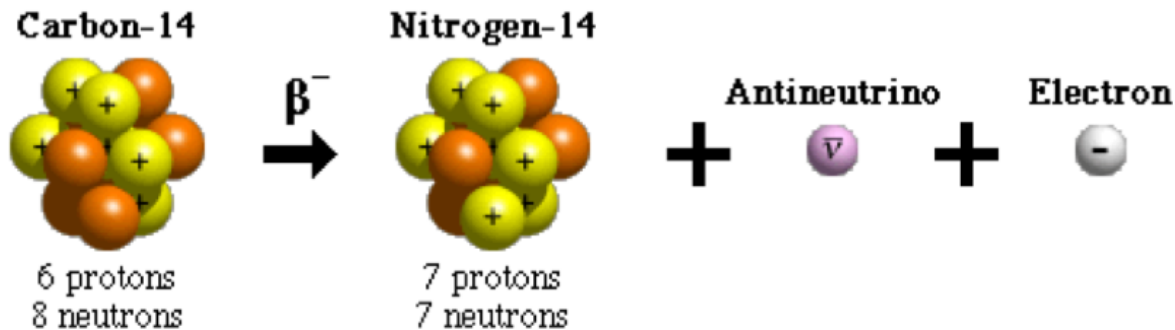




Beta Decay Examples

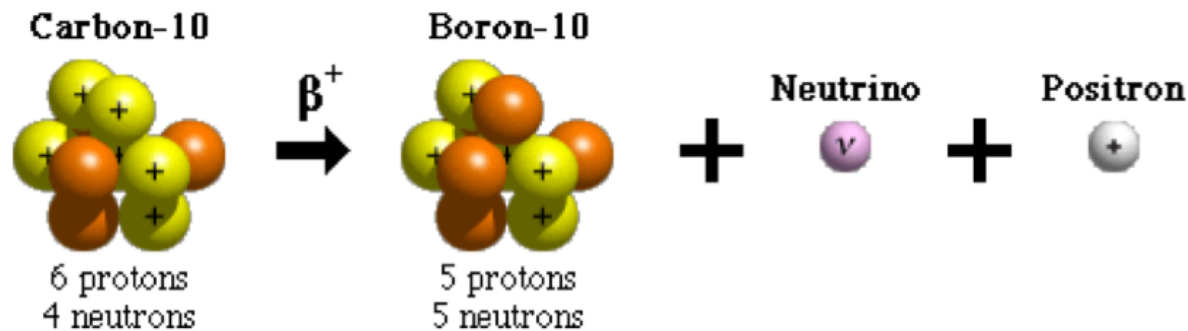
- β^- decay: $n \rightarrow p + \bar{\nu}_e + e^-$
- Moves nuclei up the periodic table ($Z \rightarrow Z + 1$)

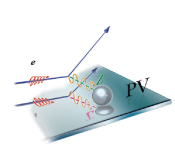
Beta-minus Decay



- β^+ decay: $p \rightarrow n + \nu_e + e^+$
- Moves nuclei down in the periodic table ($Z \rightarrow Z - 1$)

Beta-plus Decay

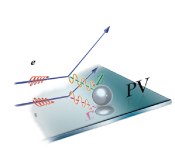




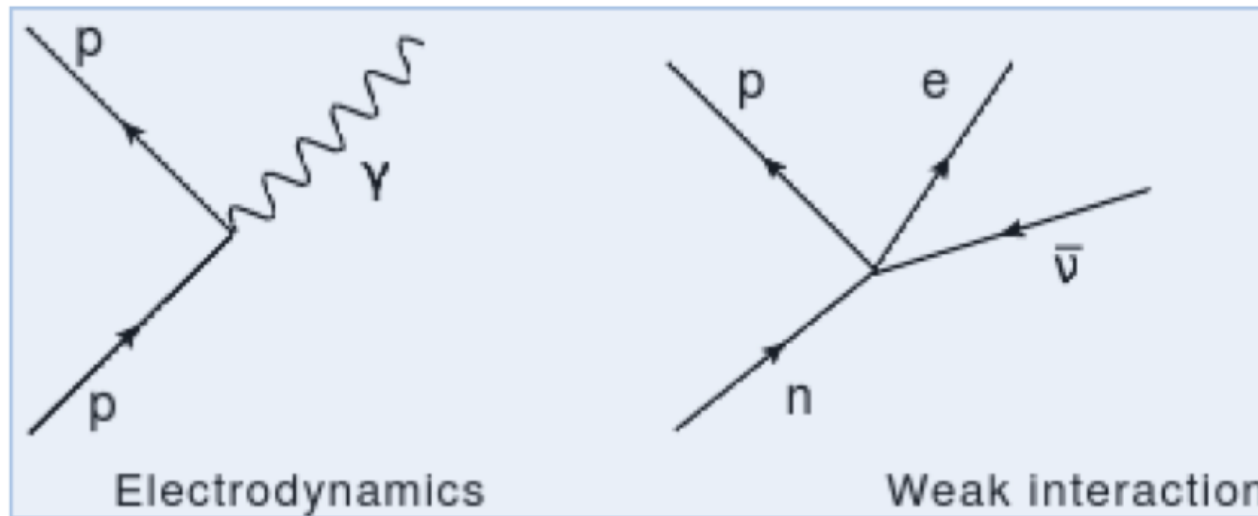
Beta Decay – Nature’s Window into the Weak-nuclear Force

A Quick History:

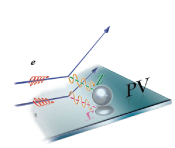
- 1899 Rutherford Rutherford classifies three types of radioactive emissions: alpha, beta, and gamma
- 1931 Pauli postulates existence of neutrino to explain non-discrete energy spectra of β -decay electrons
- 1933 Fermi develops theory to explain β decay -- precursor to theory for weak interaction
- 1956 Neutrino discovered by experiment. $\bar{\nu}_e + p \rightarrow n + e^+$
- 1957 Parity Violation discovered in β decay of ^{60}Co



Fermi's Interaction – Precursor to Weak Theory



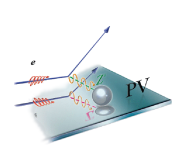
- Fermi's theory invented a physical mechanism for β decay
- 4-fermion contact interaction at single space-time point
- Modeled after electrodynamic field interactions -- where \vec{J}_E of a charged particle interacts with \vec{A} to create a photon
- For Fermi's theory, the ``weak'' current of pn-pair interacts with the ``weak'' current of $e\bar{\nu}$ -pair
- Fermi's ``weak'' currents/potentials had vector form just as EM.



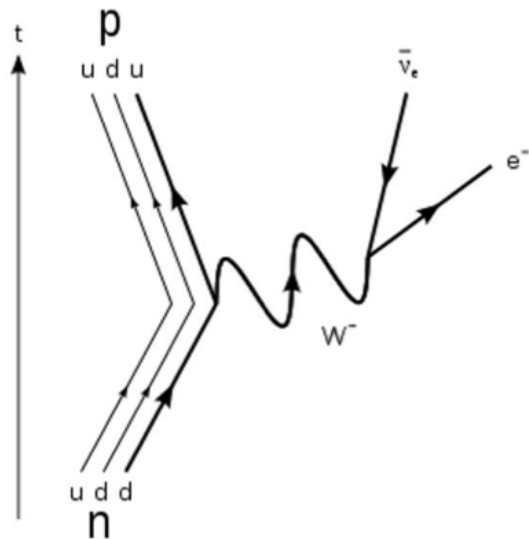
Parity Symmetry

$$\mathbf{P}: \begin{bmatrix} x \\ y \\ z \end{bmatrix} \longrightarrow \begin{bmatrix} -x \\ -y \\ -z \end{bmatrix}$$

- Parity operation: Spatial reflection through the origin
- “Even” functions: $\mathbf{P} f(x, y, z) \Rightarrow +f(x, y, z)$
- “Odd” functions: $\mathbf{P} f(x, y, z) \Rightarrow -f(x, y, z)$
- *Classically*, scalar quantities (m, E, ρ, V, M, \dots) are mainly “even” while vector quantities ($\vec{x}, \vec{a}, \vec{F}, \vec{E}, \vec{A}, \dots$) are mainly “odd”
- *Quantum Mechanically*, if \mathbf{P} commutes with the Hamiltonian, then Parity is conserved (invariant or symmetric)
- Fundamental symmetry of nature known to be conserved in electromagnetism, strong interactions, and gravity

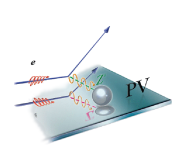


β^- Decay and Standard Model



	mass → $\approx 2.3 \text{ MeV}/c^2$ charge → $2/3$ spin → $1/2$ u up	mass → $\approx 1.275 \text{ GeV}/c^2$ charge → $2/3$ spin → $1/2$ c charm	mass → $\approx 173.07 \text{ GeV}/c^2$ charge → $2/3$ spin → $1/2$ t top	mass → 0 charge → 0 spin → 1 g gluon	mass → $\approx 126 \text{ GeV}/c^2$ charge → 0 spin → 0 H Higgs boson
QUARKS	mass → $\approx 4.8 \text{ MeV}/c^2$ charge → $-1/3$ spin → $1/2$ d down	mass → $\approx 95 \text{ MeV}/c^2$ charge → $-1/3$ spin → $1/2$ s strange	mass → $\approx 4.18 \text{ GeV}/c^2$ charge → $-1/3$ spin → $1/2$ b bottom	mass → 0 charge → 0 spin → 1 γ photon	
	mass → $0.511 \text{ MeV}/c^2$ charge → -1 spin → $1/2$ e electron	mass → $105.7 \text{ MeV}/c^2$ charge → -1 spin → $1/2$ μ muon	mass → $1.777 \text{ GeV}/c^2$ charge → -1 spin → $1/2$ τ tau	mass → $91.2 \text{ GeV}/c^2$ charge → 0 spin → 1 Z Z boson	GAUGE BOSONS
LEPTONS	mass → $< 2.2 \text{ eV}/c^2$ charge → 0 spin → $1/2$ ν_e electron neutrino	mass → $< 0.17 \text{ MeV}/c^2$ charge → 0 spin → $1/2$ ν_μ muon neutrino	mass → $< 15.5 \text{ MeV}/c^2$ charge → 0 spin → $1/2$ ν_τ tau neutrino	mass → $80.4 \text{ GeV}/c^2$ charge → ± 1 spin → 1 W W boson	

- Julian Schwinger modifies Fermi's theory to incorporate parity violating potential term (V-A) and idea of intermediate vector bosons; Glashow, Weinberg, and Salam 1979 Nobel Prize
- W^\pm only couples to left-handed particles and right-handed anti-particles
- Z^0 couples predominantly to left-handed particles

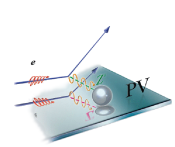


Why Parity-Violating Electron Scattering?

Provides model-independent determinations of nuclear and fundamental-particle weak-charge form factors and couplings with widespread implications for:

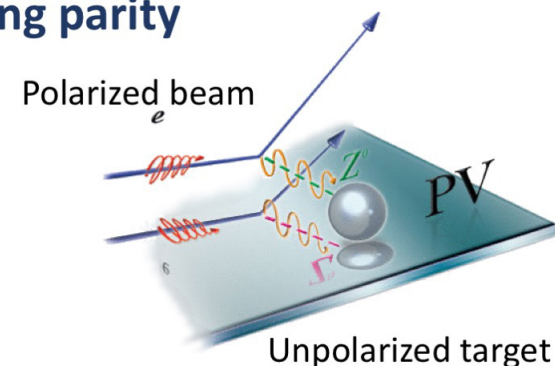
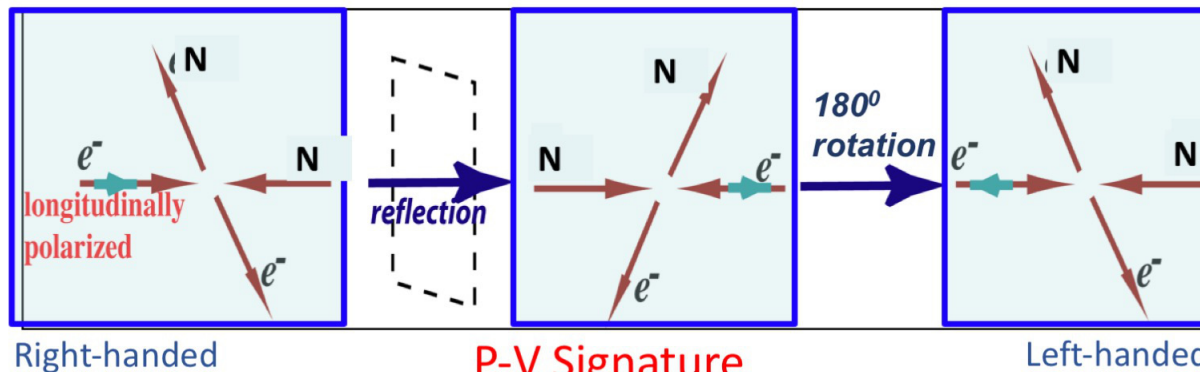
- Understanding nuclear and nucleon structure
 - Strange quark content of nucleon
 - Neutron radii of heavy nuclei \rightarrow density dependence of Symmetry Energy and EOS of nuclear matter; neutron stars; calibrate hadronic probe reactions on radioactive beams
- Search for physics Beyond the Standard Model (BSM)
 - Indirect searches using low energy ($Q^2 \ll M_Z^2$) precision electroweak tests at high intensity or precision frontier
 - complements direct searches at high energy frontier

JLab PVES Programs: HAPPEX, G0, PVDIS, PREX, Qweak, CREX
MOLLER, SoLID



Parity-Violating Electron Scattering

Parity Transformation: Changing beam helicity equivalent to changing parity



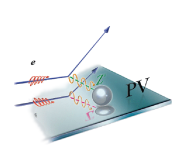
$$\sigma \approx \left| \begin{array}{c} \text{diagram with } \gamma \\ \text{diagram with } z^0 \end{array} \right|^2$$

- Access NC Weak amplitude via **EW interference**-dominated asymmetry measurement

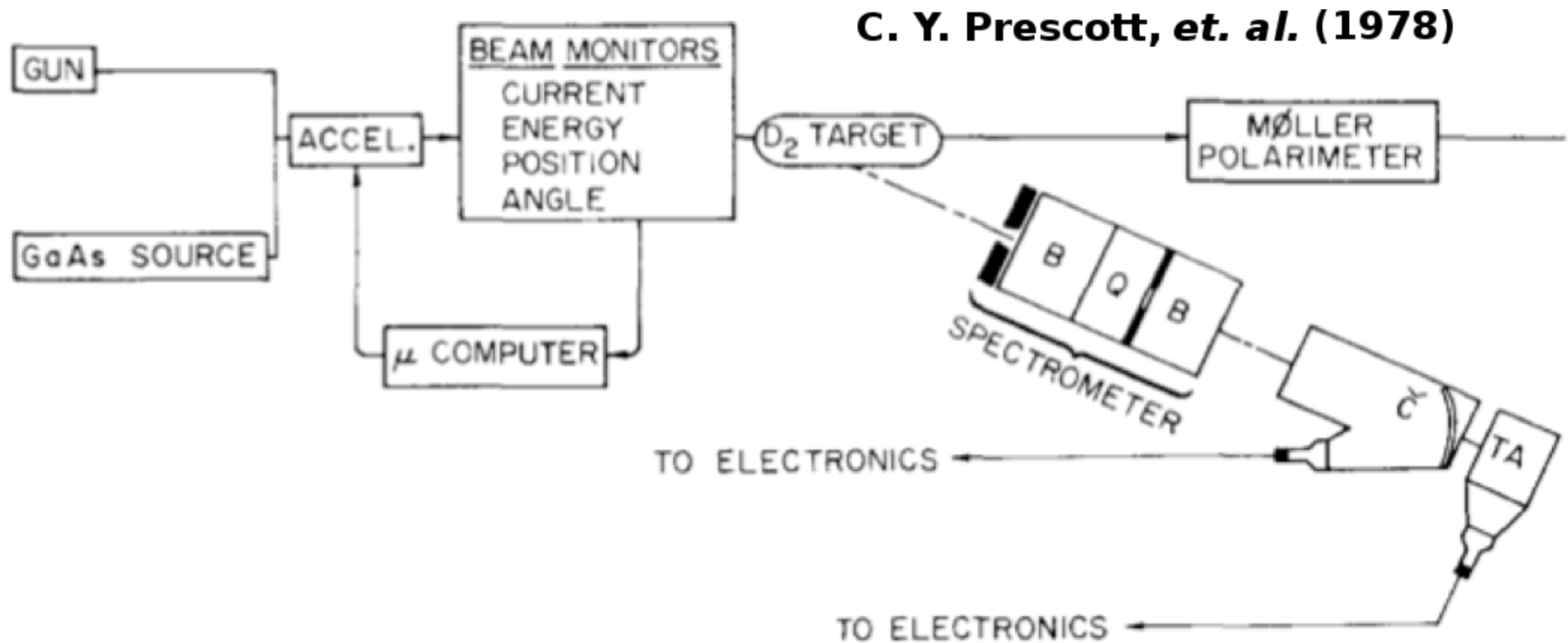
$$= \left| \begin{array}{c} \text{diagram with } \gamma \\ \text{diagram with } z^0 \end{array} \right|^2 + h_e \left| \begin{array}{c} \text{diagram with } \gamma \\ \text{diagram with } z^0 \end{array} \right| + \left| \begin{array}{c} \text{diagram with } z^0 \end{array} \right|^2$$

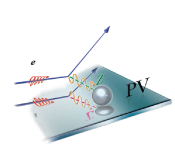
- Flip sign of longitudinal polarization
- Measure fractional rate difference or **asymmetry**

$$A_{PV} = \frac{\sigma_R - \sigma_L}{\sigma_R + \sigma_L} \approx \frac{M_{Weak}^{NC}}{M_{EM}} \approx \frac{G_F Q^2}{4\pi\alpha} \sim 10^{-4} \cdot Q^2 \text{ [}/GeV^2]$$

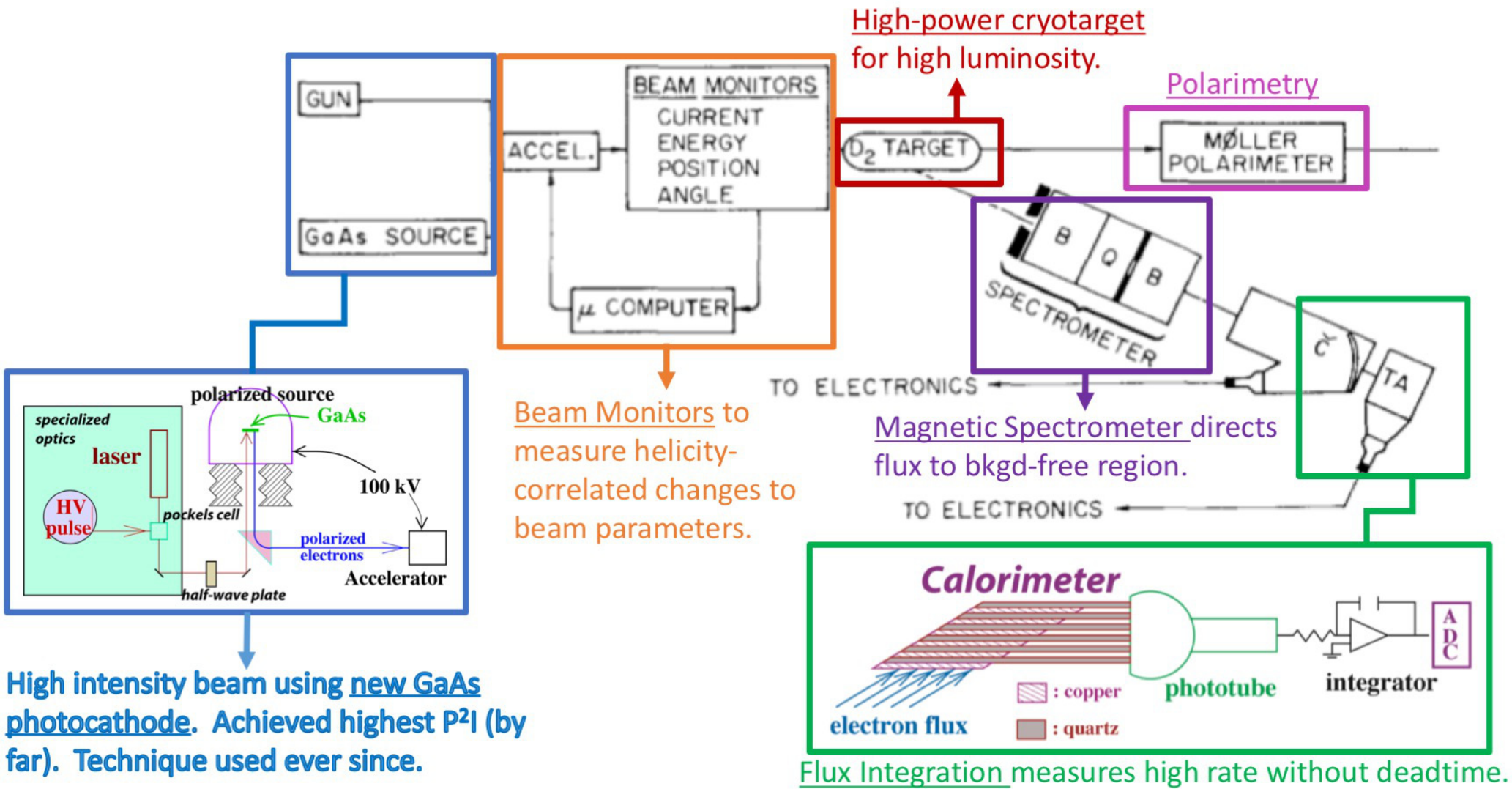


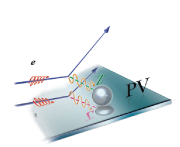
Blueprint of a PVES Experiment (E122 at SLAC)



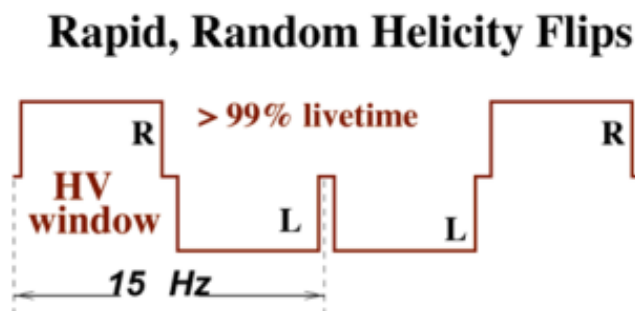
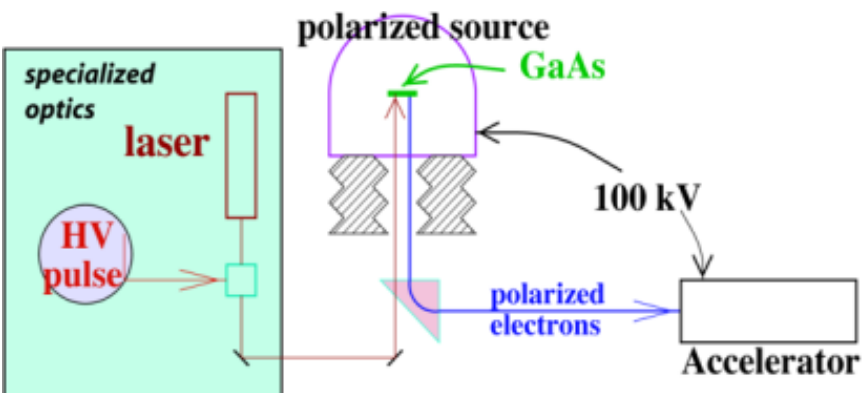


Anatomy of a PVES Experiment (E122 at SLAC)





How to do a Parity Experiment



Measure flux F for each window

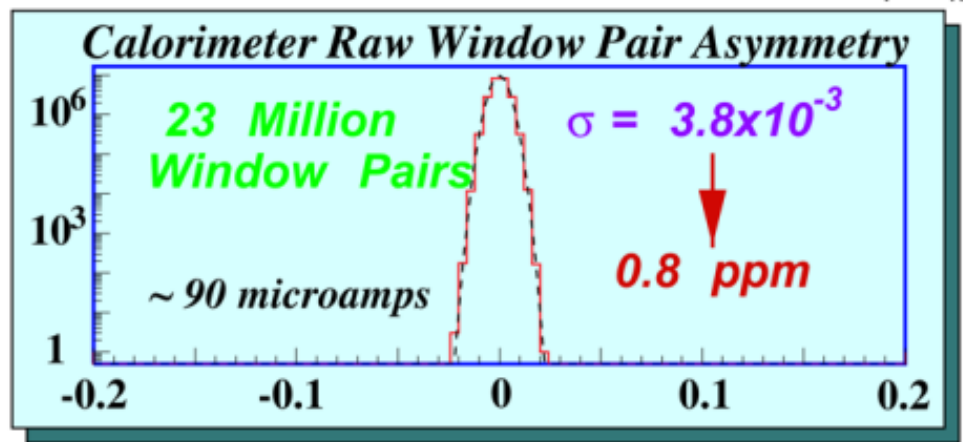
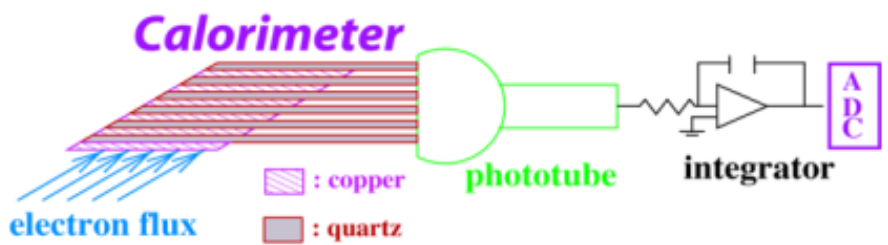
$$A_{\text{window pair}} = \frac{F_R - F_L}{F_R + F_L}$$

rapid, random, helicity flipping

Flux Integration Technique:

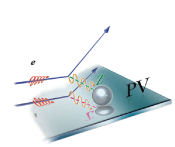
- HAPPEX: 2 MHz ($A_{PV} \sim 15\text{ppm}$)
- HAPPEX-II: 100 MHz ($A_{PV} \sim 1.5\text{ppm}$)
- PREX: 1 GHz ($A_{PV} \sim 0.5\text{ppm}$)
- PREX-II: 2 GHz ($A_{PV} \sim 0.5\text{ppm}$)
- MOLLER: 150 GHz ($A_{PV} \sim 0.035\text{ppm}$)

Signal Average N Windows Pairs: $A \pm \frac{\sigma(A)}{\sqrt{N_{\text{windows}}}}$



No non-gaussian tails to +/- 5σ

Detector signal noise dominated by electron counting statistics



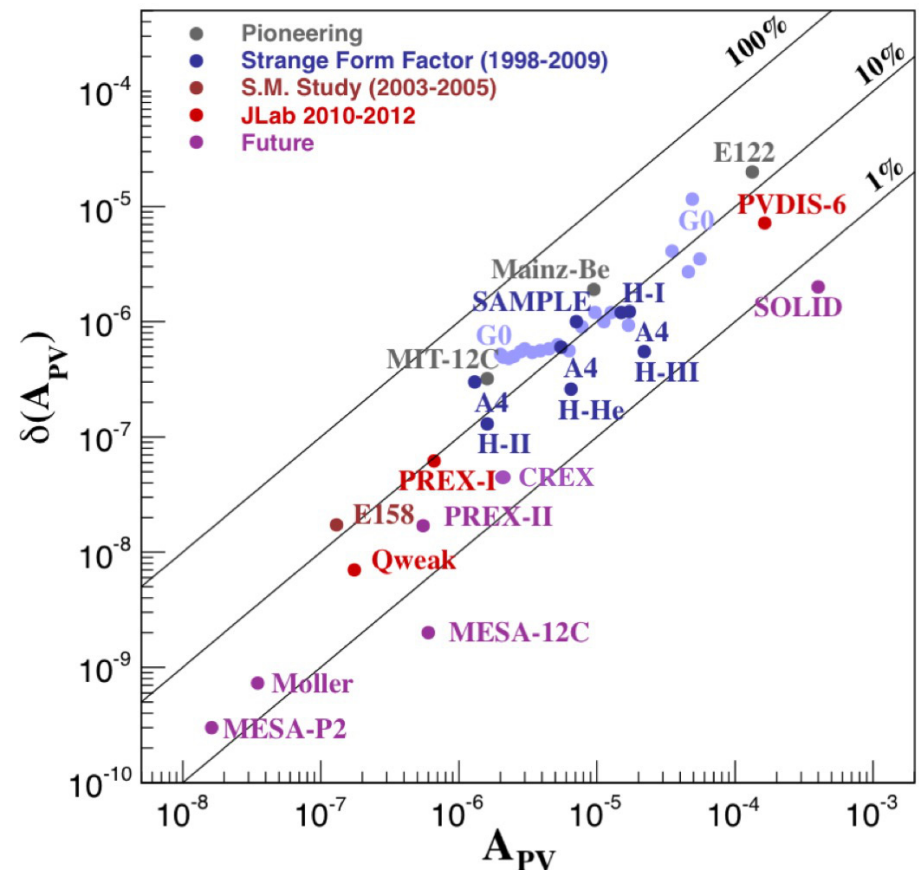
3 Decades of Technical Progress

photocathodes, polarimetry, high power cryotargets, nanometer beam stability, precision beam diagnostics, low noise electronics, *rad-hard dets*

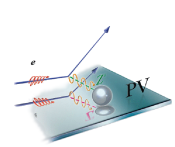
- 1st generation
- 2nd generation
- 3rd generation
- 4th generation

E122 – 1st PVES Expt (late 70’s at SLAC)
 Mainz & MIT-Bates in mid 80’s
 JLab program launched in mid 90’s
 E158 at SLAC meas PV Møller scattering
 MOLLER at JLab in mid 2020’s

PVES Experiment Summary

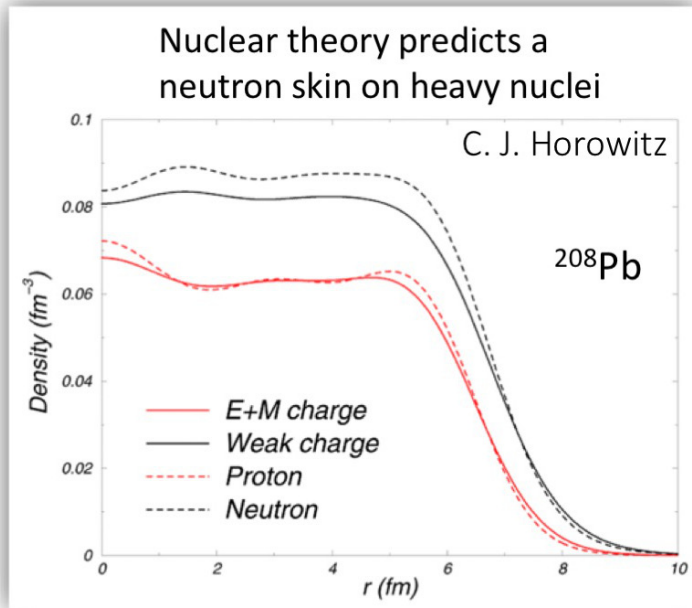


- Parity-violating electron scattering has become a precision tool!



PREX/CREX Concept

(Probing the Weak Charge Distribution of N-rich Nuclei)



Present knowledge of neutron distributions comes primarily from hadron scattering → model-dependent interpretation, large and uncontrolled uncertainties

- ❖ Parity violation can measure neutron and weak-charge form factors *model-independently* with *statistics-dominated uncertainty*

$$M_{EM} = \frac{4\pi\alpha}{Q^2} F_p(Q^2) \quad \left(\begin{array}{l} \text{EM amplitude accesses charge} \\ \text{or proton form factor} \end{array} \right)$$

$$M_{Weak}^{NC} = \frac{G_F}{\sqrt{2}} \left[\underbrace{(1 - 4\sin^2\theta_W)}_{Q_W^p \sim 0} F_p(Q^2) - F_n(Q^2) \right]$$

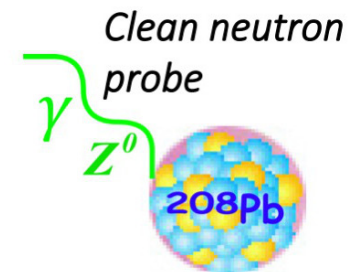
\downarrow
 $Q_W^n \simeq -1$

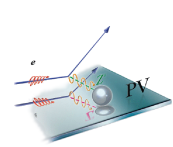
	Proton	Neutron
Electric Charge	1	0
Weak Charge	~0.08	-1

- Neutron distribution not accessible to the charge-sensitive photon
- Z^0 couples primarily to neutron

$$A_{PV} \approx \frac{G_F Q^2}{4\pi\alpha\sqrt{2}} \frac{F_n(Q^2)}{F_p(Q^2)}$$

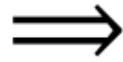
$$F_{n,p}(Q^2) = \frac{1}{4\pi} \int d^3r j_0(qr) \rho_{n,p}(r)$$



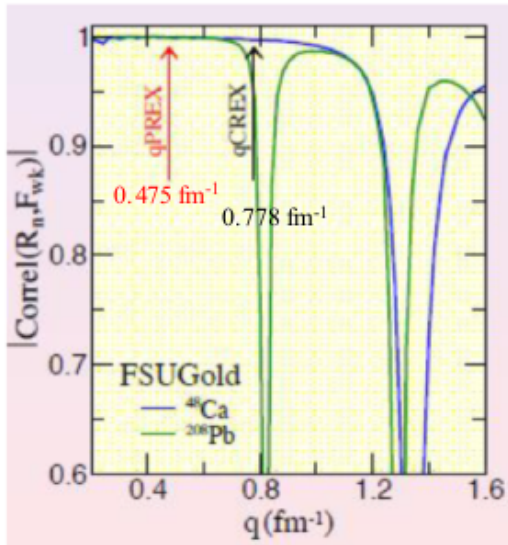


PREX/CREX Concept

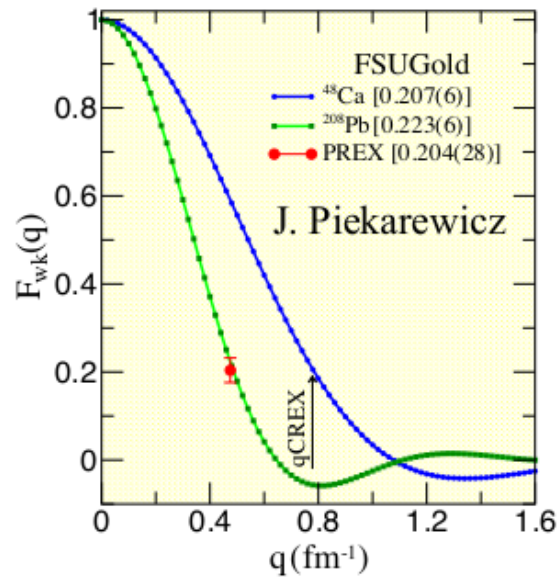
At low Q^2 there is a tight correlation between R_n and $F_{wk}(Q^2)$



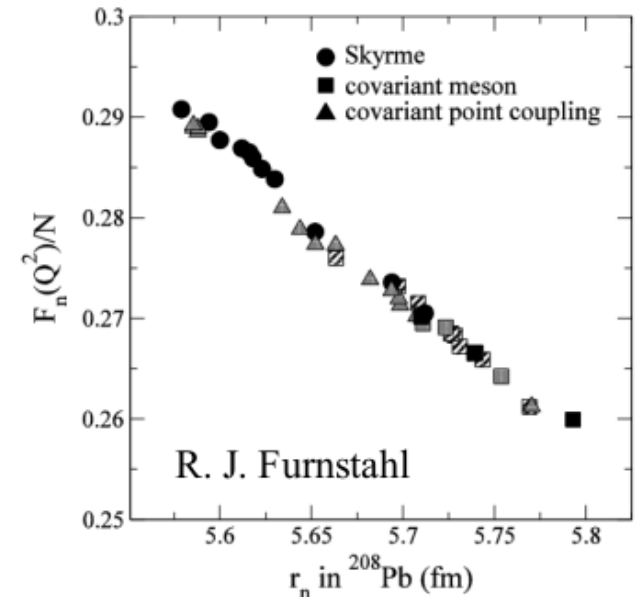
A single measurement of $F_{wk,n}(Q^2)$ translates to a measurement of R_n (via mean-field nuclear models)



Relativistic Mean-field
EDF covariant analysis



J. Piekarewicz



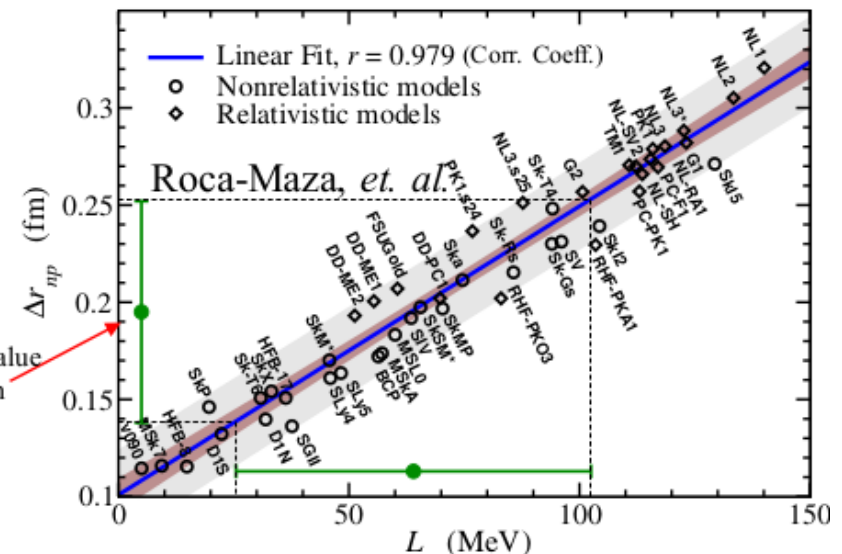
R. J. Furnstahl

- Energy Density Functions (EDFs) characterized by a dozen free parameters that are calibrated to a host of well known properties of finite nuclei

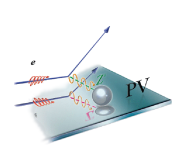
❖ There is a strong correlation between R_n and the density dependence or slope of the symmetry energy,

$$L = 3\rho_0 \left(\frac{\partial S}{\partial \rho} \right)_{\rho_0}$$

Arbitrary central value with PREX 0.06 fm proposed errorbar



At present, L is not well constrained by “Real” data!



PREX/CREX Overview

PREX/PREX-II:

0.95 GeV e⁻ beam, 50-70 μA

0.5 mm thick ²⁰⁸Pb target

5° scattered electrons

$Q^2 = 0.0088 \text{ GeV}^2$, $A_{PV} \sim 0.5 \text{ ppm}$

680 hours, ~35M pairs

$\delta A_{PV} \sim 15 \text{ ppb}$ (3%)

- high polarization, ~89%
- helicity reversal at 240 & 30 Hz

CREX:

2.22 GeV e⁻ beam, 150 μA

5 mm thick ⁴⁸Ca target

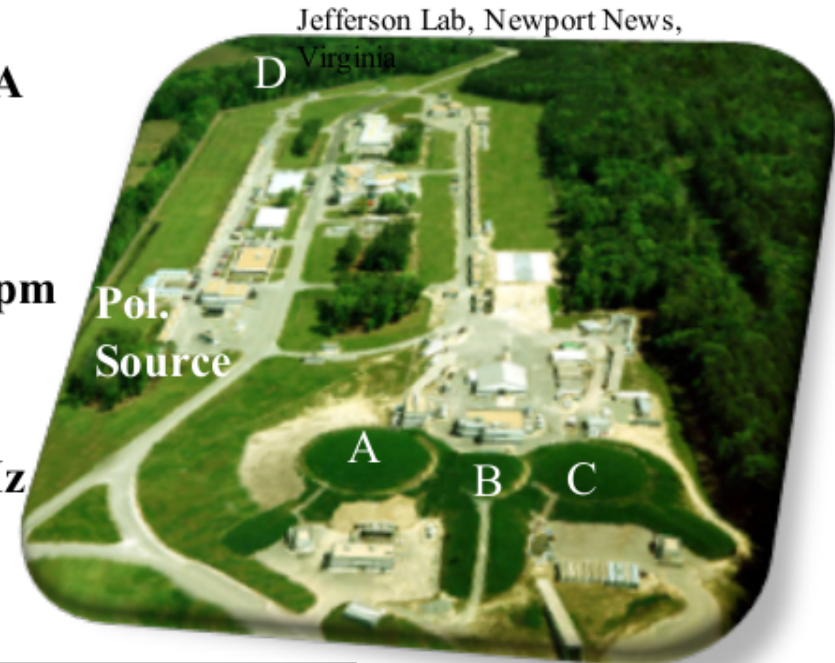
5° scattered electrons

$Q^2 = 0.037 \text{ GeV}^2$, $A_{PV} \sim 2 \text{ ppm}$

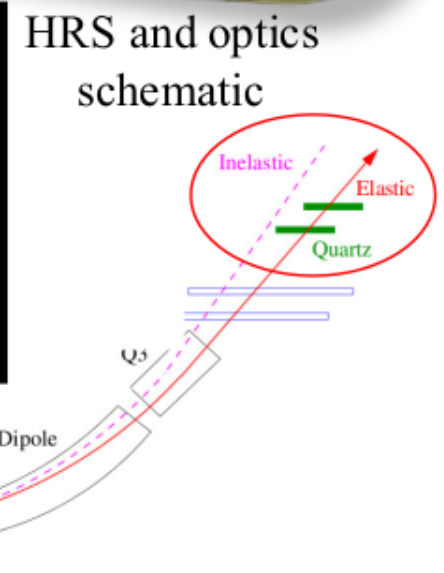
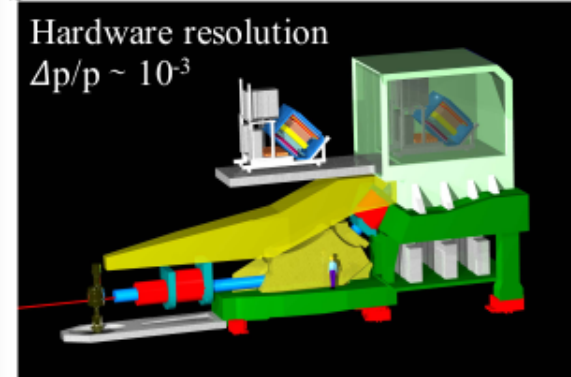
780 hours, ~40M pairs

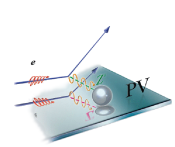
$\delta A_{PV} \sim 80 \text{ ppb}$ (4%)

- **New thin quartz detectors**



Symmetric High Resolution Spectrometers

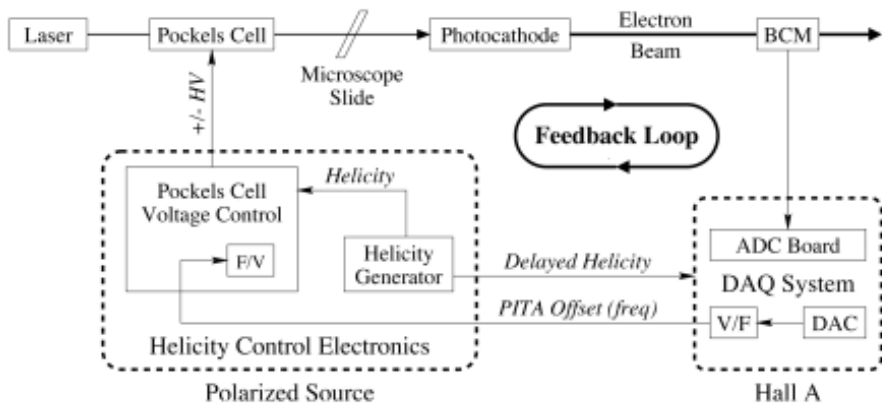




”Parity Quality” Beam Monitoring

(normalization and false-asymmetry systematics control)

• Precision source-laser alignment



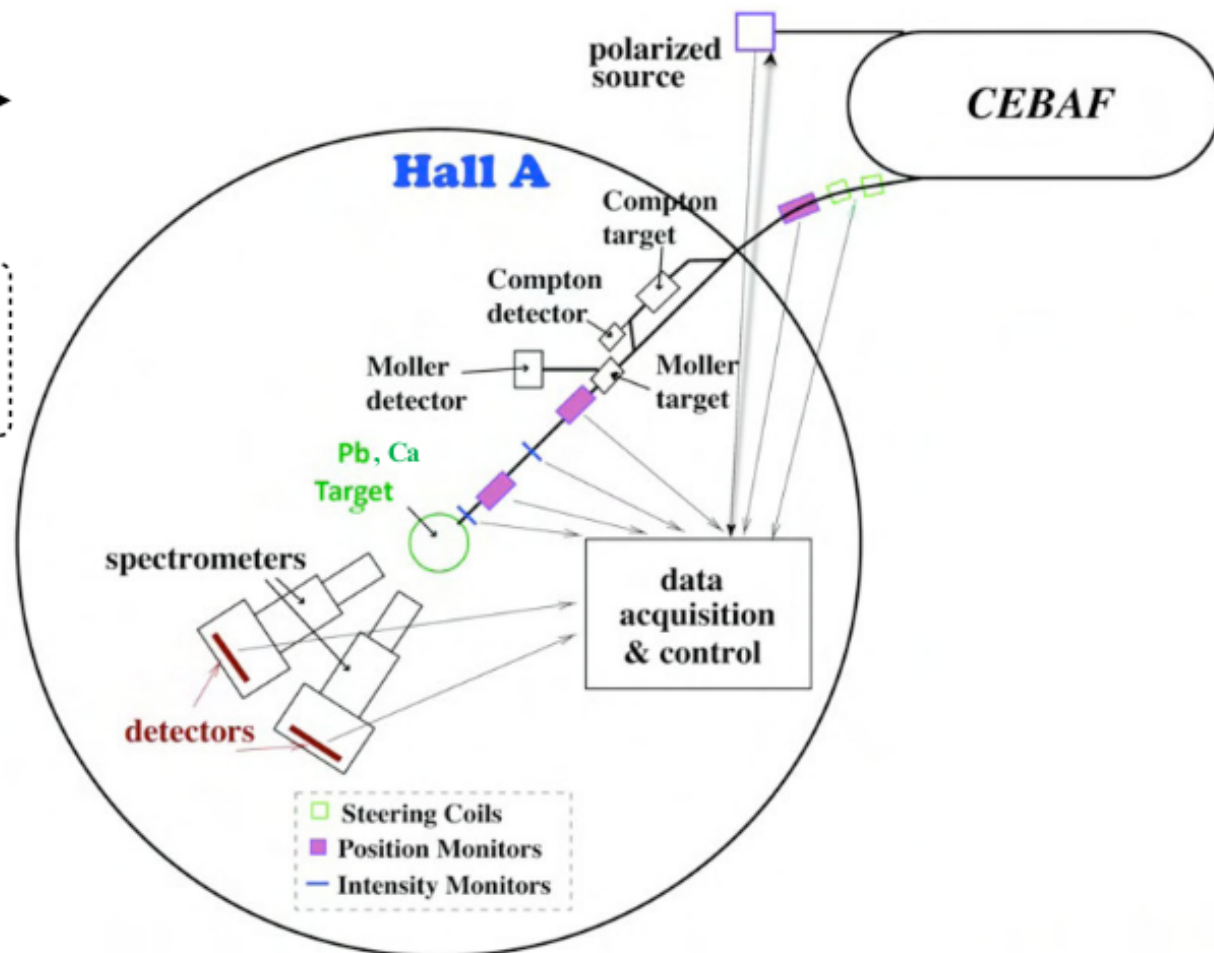
• Active feedback on charge asymmetry

• Precision beam position monitoring with active calibration of detector slopes (via beam modulation)

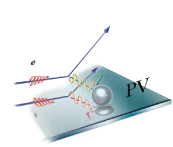
• Two independent methods for “slow” helicity reversals:

1. Insertable half-wave plate
2. Double Wien filter

• Continuous beam polarization monitoring with Compton polarimeter



Hall A Parity Quality Beam Monitoring Schematic



PREX-I Systematic Errors

PREX goal for ~ 2% total systematic error achieved!

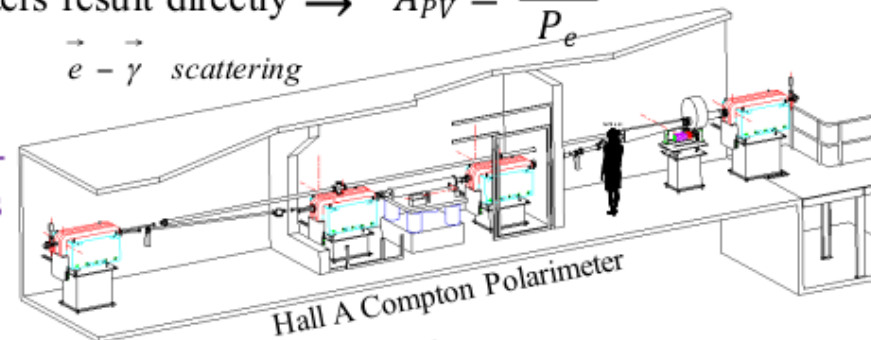
Systematic Error	Absolute (ppm)	Relative (%)
Polarization	0.0083	1.3
Detector Linearity	0.0076	1.2
Beam current normalization	0.0015	0.2
Rescattering	0.0001	0
Transverse Polarization	0.0012	0.2
Q^2	0.0028	0.4
Target Backing	0.0026	0.4
Inelastic States	0	0
TOTAL	0.0140	2.1

Crucial normalizations:

- Polarization:** enters result directly $\rightarrow A_{PV} = \frac{A_{raw}}{P_e}$

$\vec{e} - \vec{\gamma}$ scattering

Use Compton Polarimetry for non-invasive, continuous measurement



Hall A Compton Polarimeter

- 4-momentum transfer:** $Q^2 = 4EE' \sin^2 \frac{\theta}{2}$

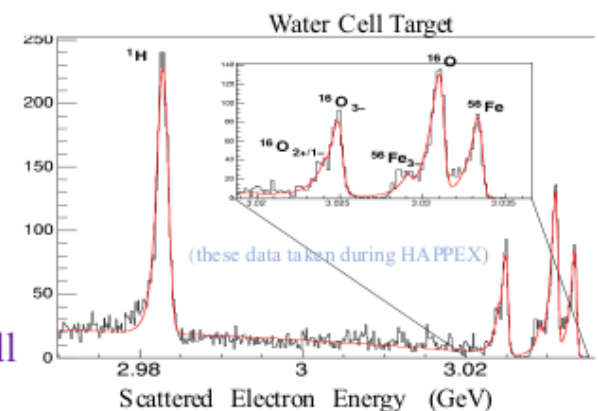
Calibrations:

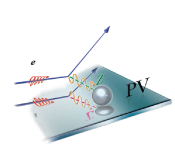
- E (beam energy): spin precession in the machine
- E' (scattered energy): NMR probe in HRS B-field
- θ (scattered angle): surveyed to ~1 mrad and measured to 0.2% absolute using water cell target

Absolute angle calibration via nuclear recoil variation

$$\delta E_{\text{loss}} \approx \frac{\theta^2}{2} \frac{E^2}{M_A}$$

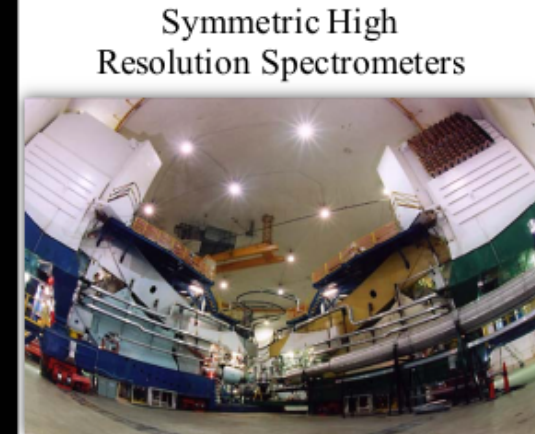
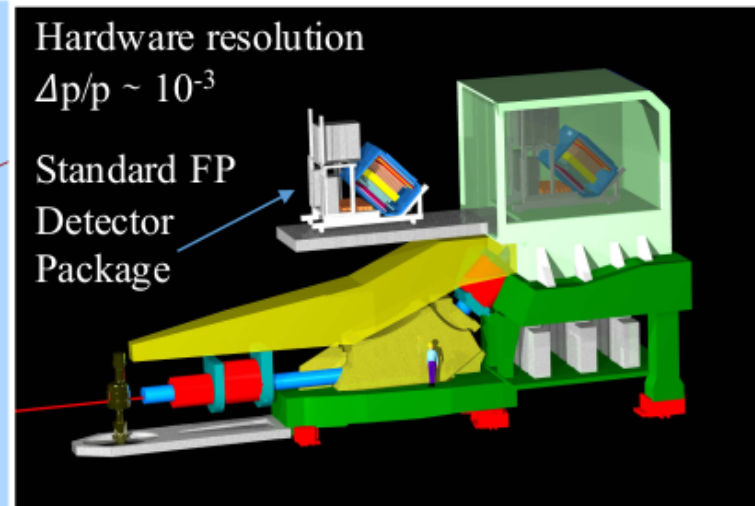
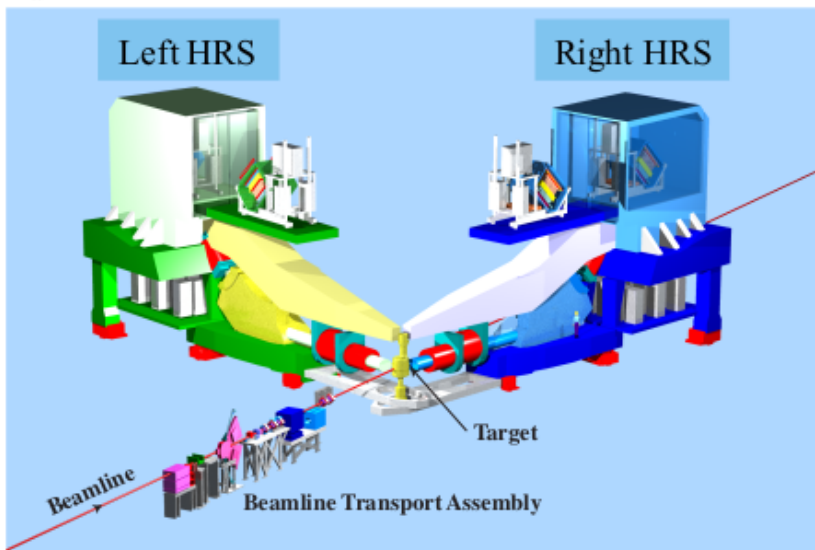
Q^2 distributions obtained by dedicated low-rate runs with tracking detectors triggered on quartz pulse-height (0.4% overall error on Q^2)





Integrating Detector Focal Plane for PV Experiments: HAPPEX through PREX-II/CREX

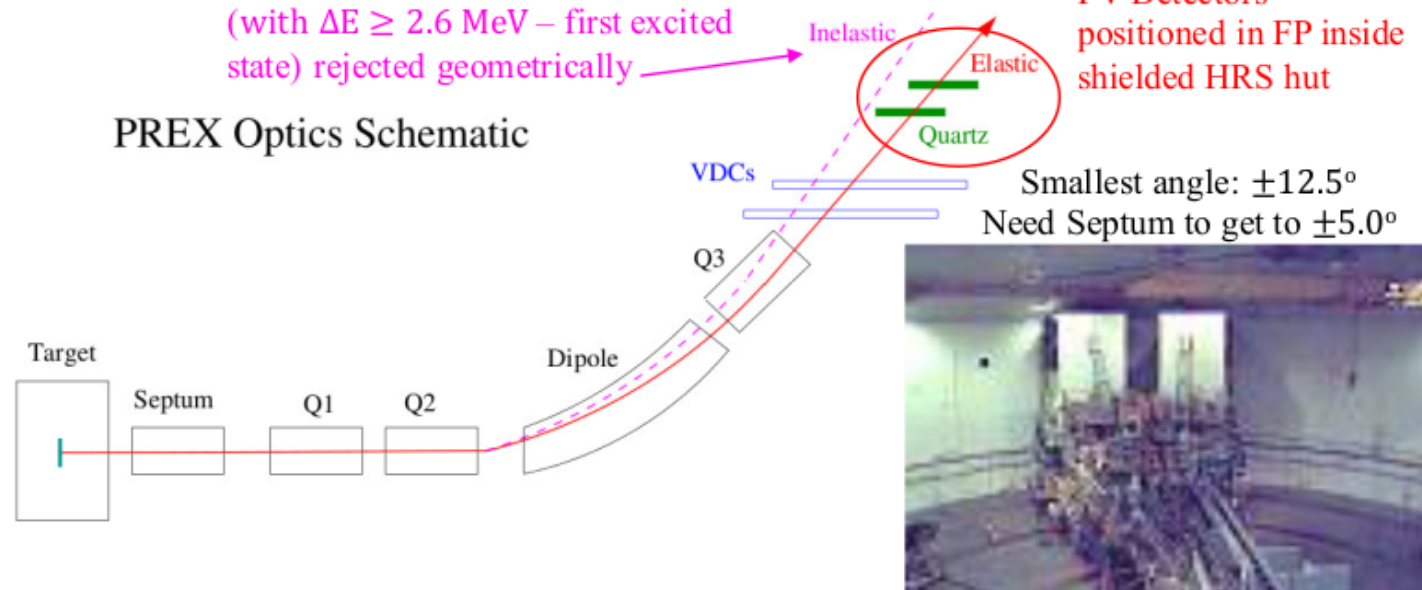
Hall A

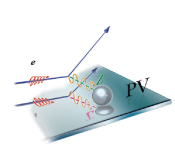


- Standard focal plane (FP) detector packages are removed during high flux PV experiments
- Specialized focal plane detectors installed and positioned to **intercept only elastically scattered electrons** – uses precision optics and hardware resolution
- Integrated PE yields from detectors are proportional to electron flux

- For PREX, inelastic events (with $\Delta E \geq 2.6$ MeV – first excited state) rejected geometrically

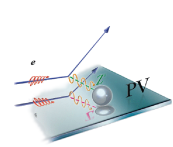
PREX Optics Schematic



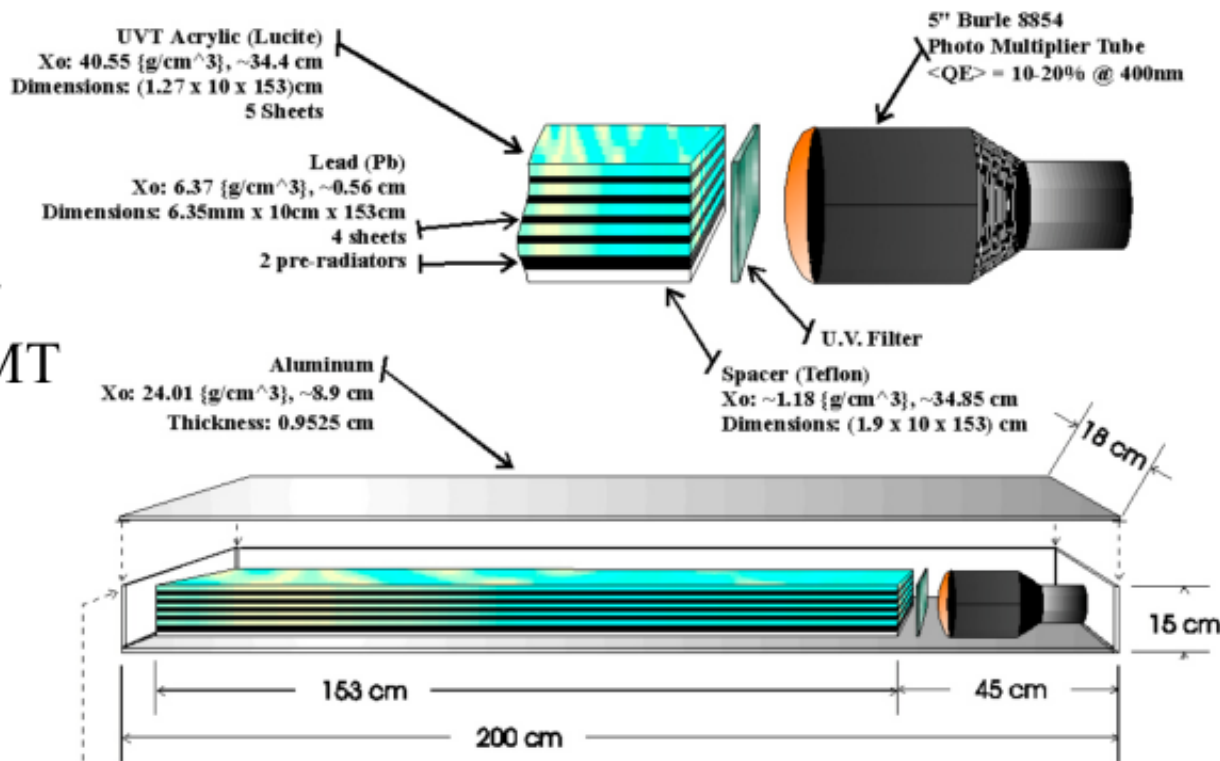


Requirements for PVES Integrating Detectors

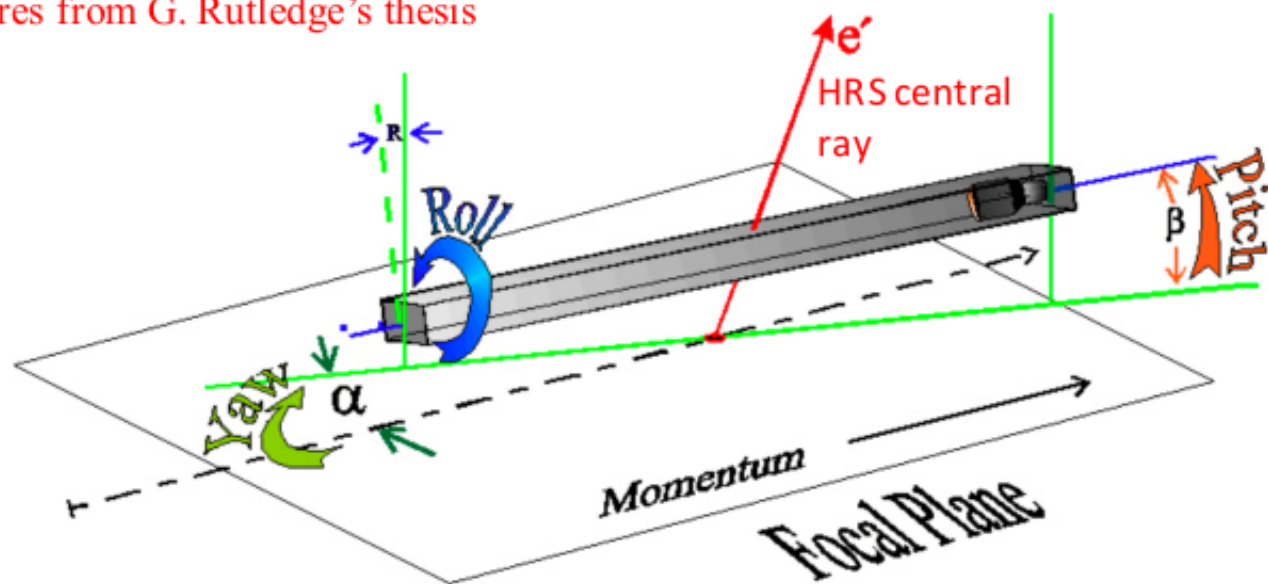
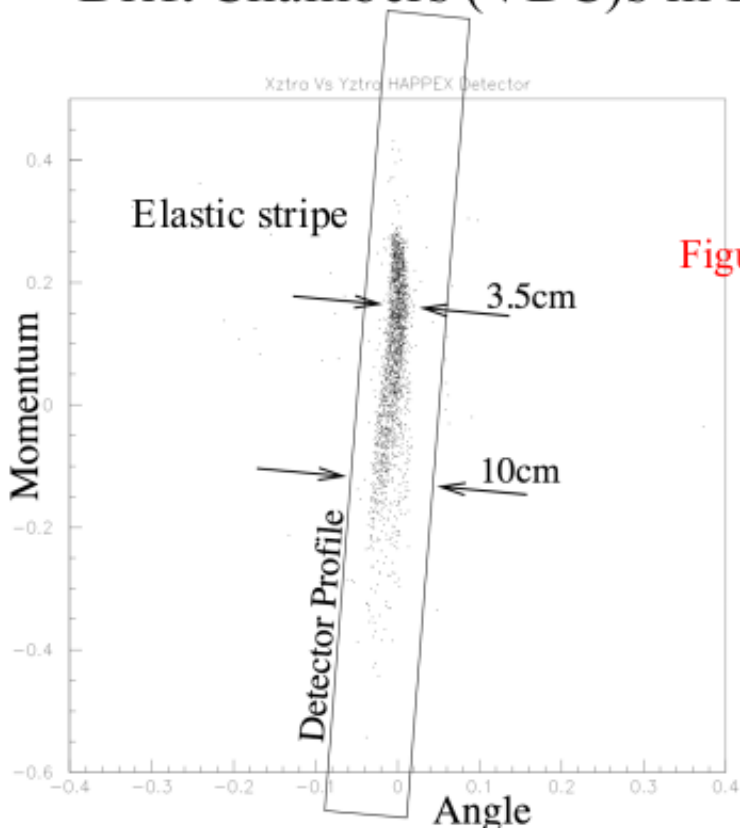
- Radiation hardness – active medium must give consistent response under extreme and prolonged flux exposures
- Should count individual electrons with good ($\sim 20\%$) resolution – to minimize statistical error inflation
- Photo-sensitive device must give highly linear response (at 0.3% level for PREX-II/CREX) – so care must be taken to understand photo-cathode light levels and anode currents during integration mode A_{PV} measurements

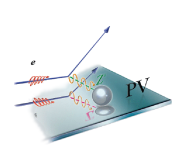


- Main integrating detector for HAPPEX, H-II, H-He, H-III
- 5 layer Pb-Acrylic calorimeter 1.5 m long with 5 inch Burl PMT
- Installed just above Vertical Drift Chambers (VDC)s in FP



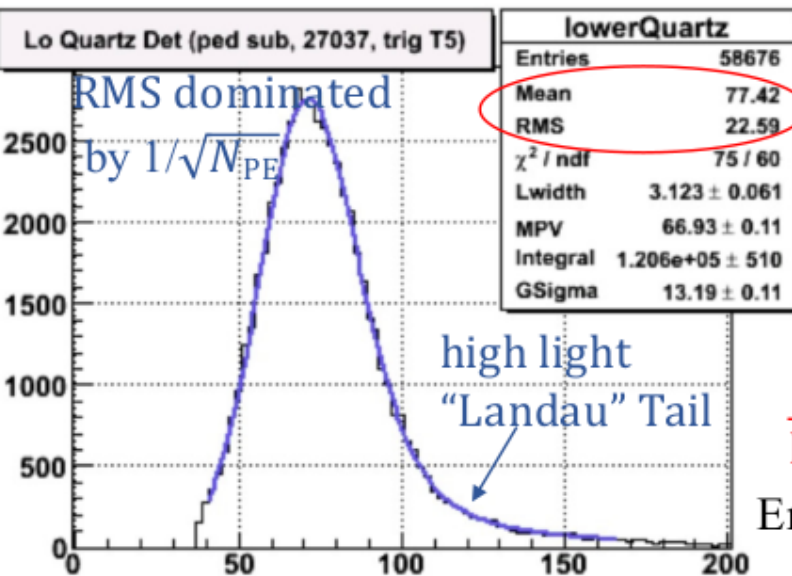
Figures from G. Rutledge's thesis





Main Integrating Detector for PREX-I (“thin” quartz Tandem Detector)

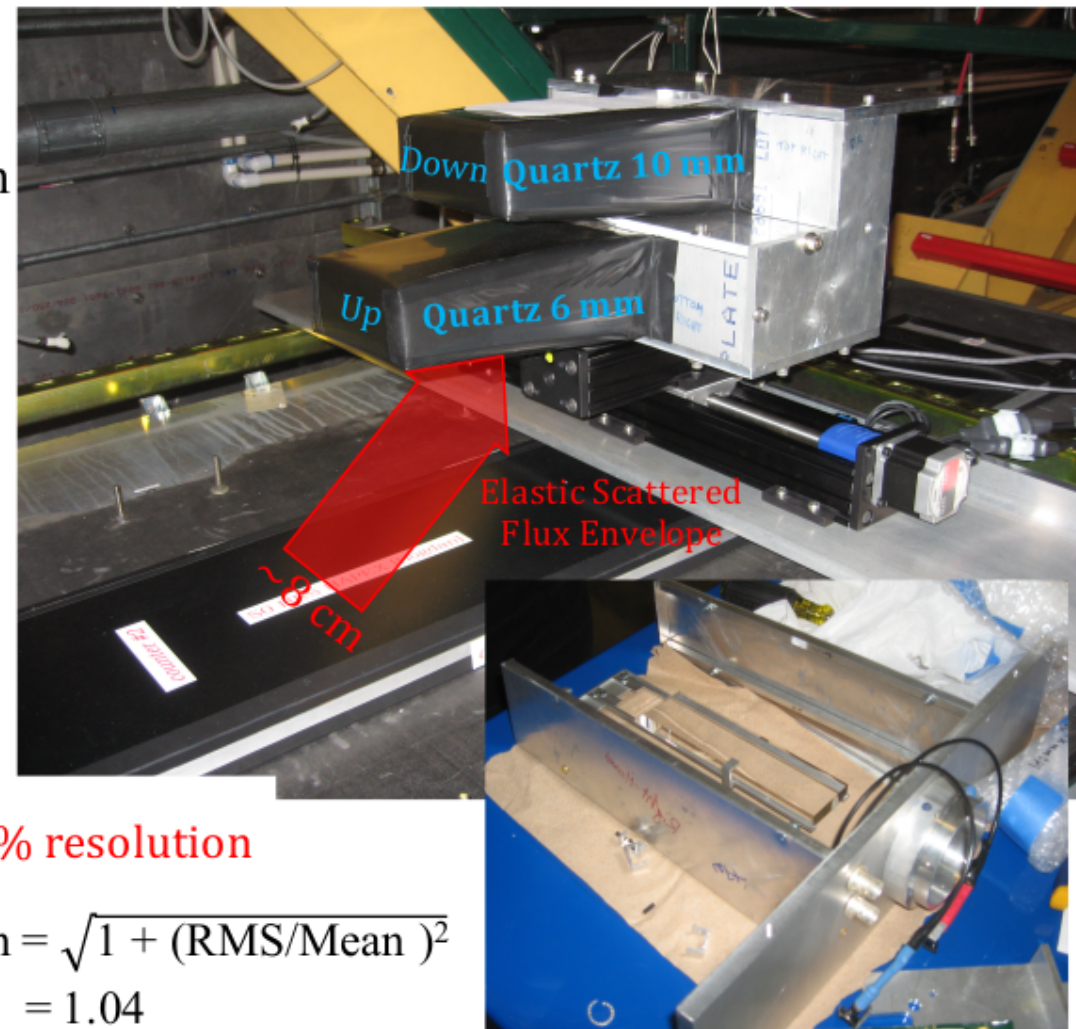
- Quartz geometry: 160 mm by 35 mm by 6 mm (upstream) and 10 mm (downstream)
- Conservative Design for PREX-I: orientation between pmt, quartz and central ray gives consistent light yields...but relatively low overall yield and okay resolution...



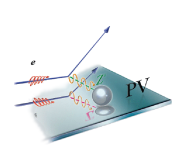
Detector ADC pulse-height distribution (acquired during “counting-mode” calibration runs)

$$\frac{\text{RMS}}{\text{Mean}} = 29\% \text{ resolution}$$

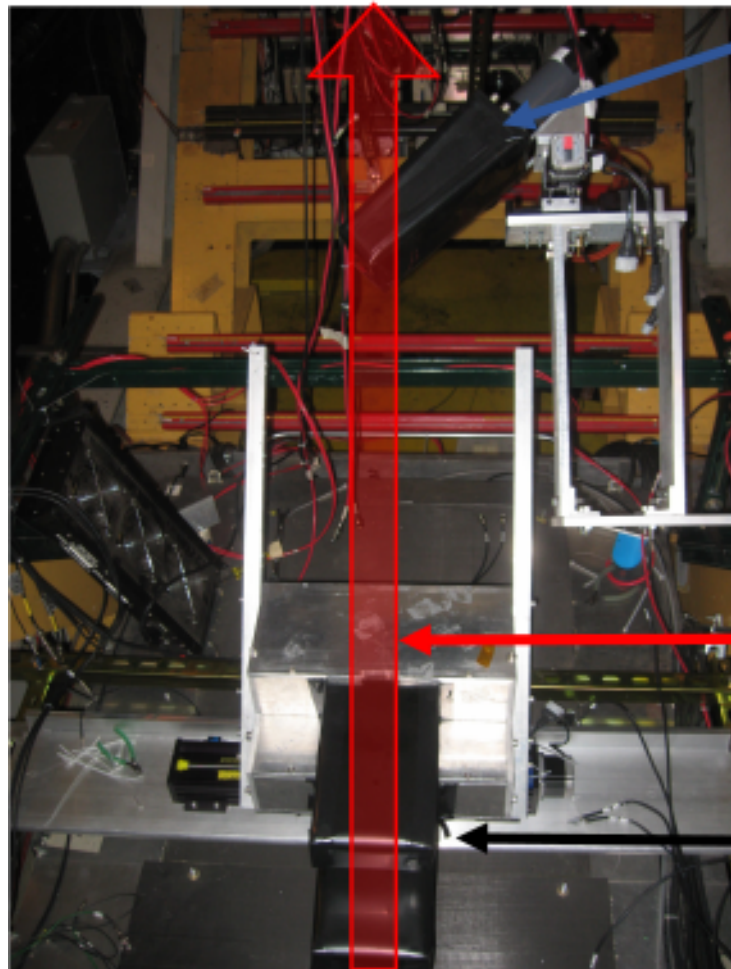
$$\text{Error Inflation} = \sqrt{1 + (\text{RMS}/\text{Mean})^2} = 1.04$$



So A_{PV} statistical error increases by ~4%



Integrating Detectors for PREX-I (Tandem and A_T Dets)



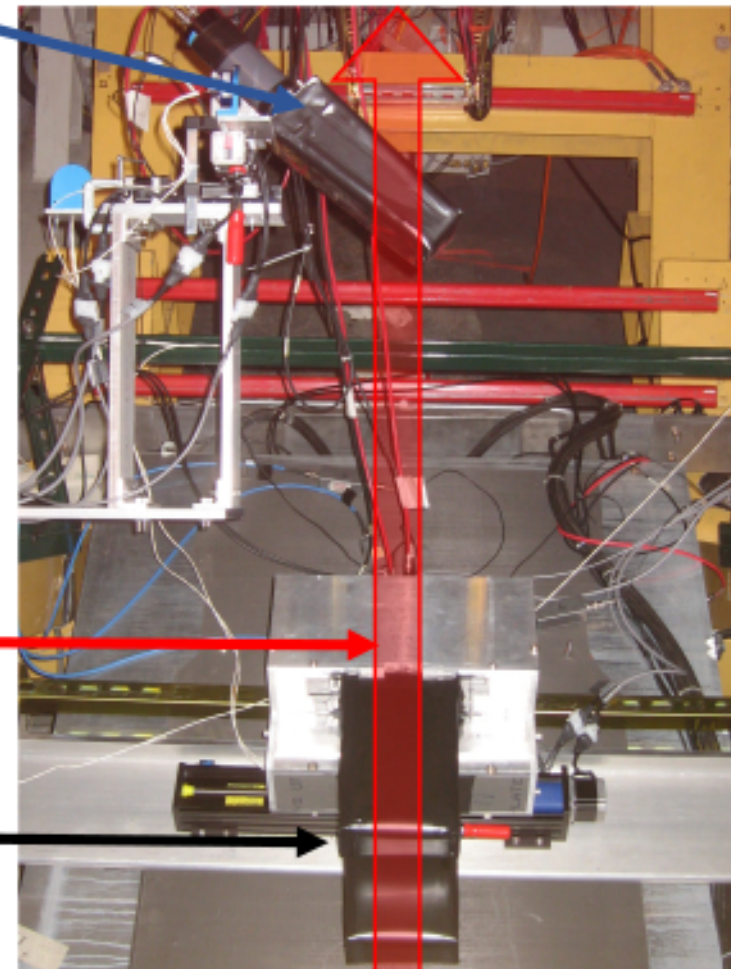
Left HRS

- A_T Detectors
 - Monitor any residual transverse beam polarization
 - Positioned to intercept larger OOP scatters (enhancing analyzing power)

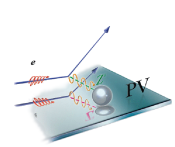
Elastic scattered flux envelopes

Main Tandem Detectors

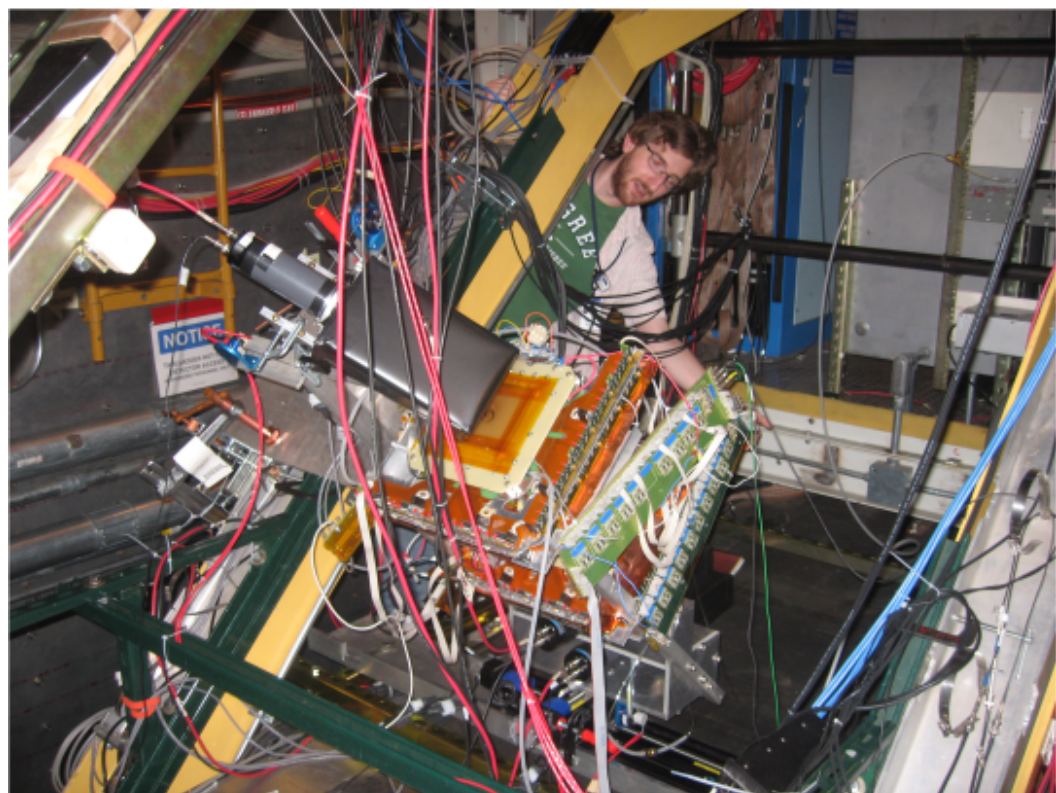
Views along dispersive \hat{x}



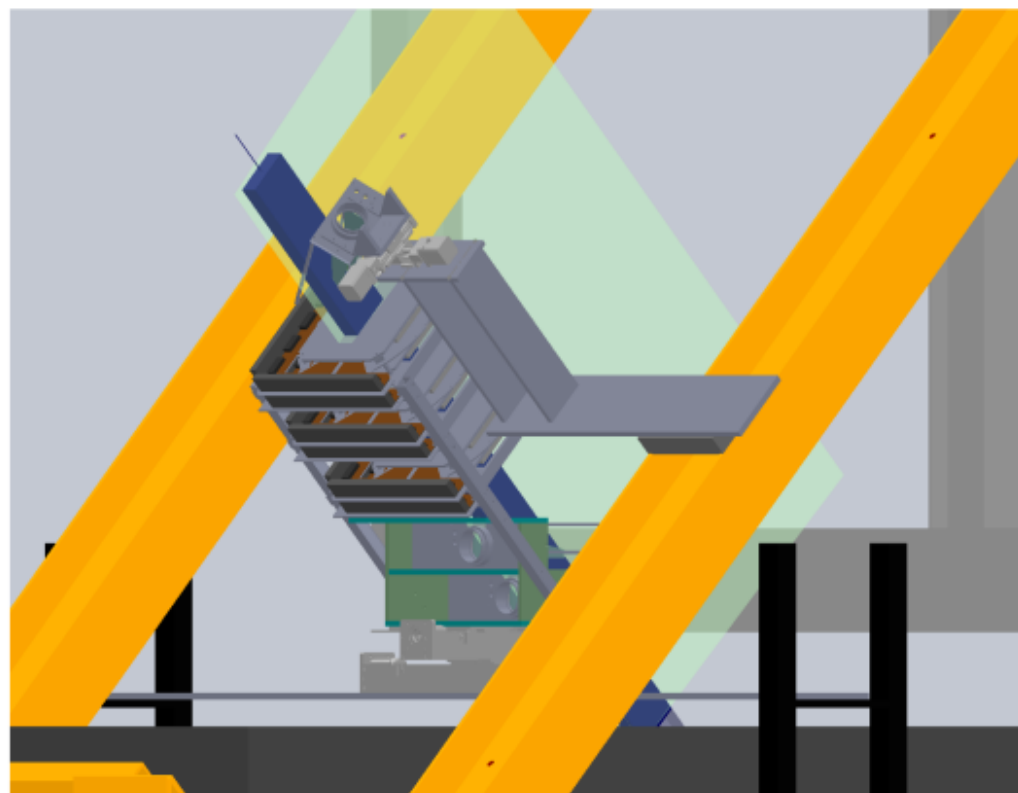
Right HRS



Integrating Detectors for PREX-I (Tandem Dets, A_T Dets and GEMs)

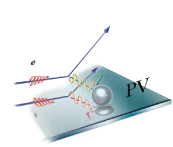


Left HRS Photo (2010)



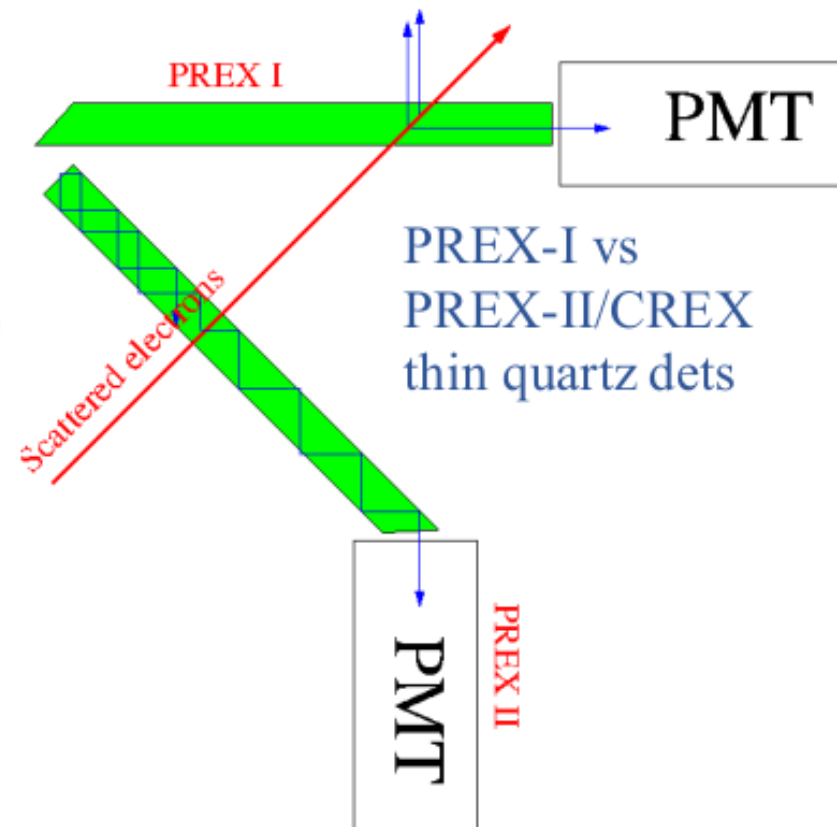
Right HRS CAD

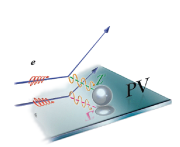
- First GEM tracking system to be used at JLab was during PREX-I; system was noisy and cumbersome
- Each HRS used three triple GEM chambers; each 10 by 10 cm² active area
- These supplement VDCs during high rate Q^2 and optics calibration runs



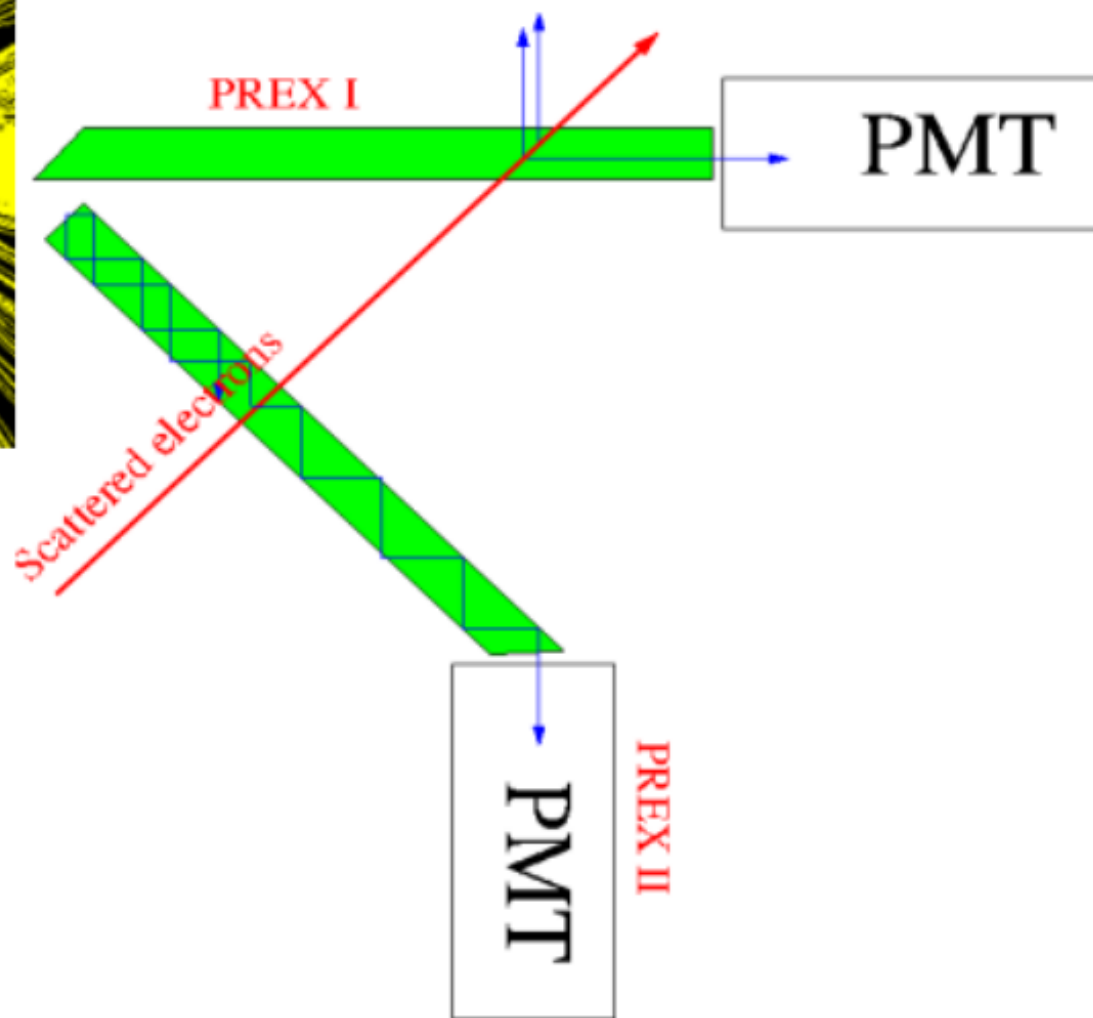
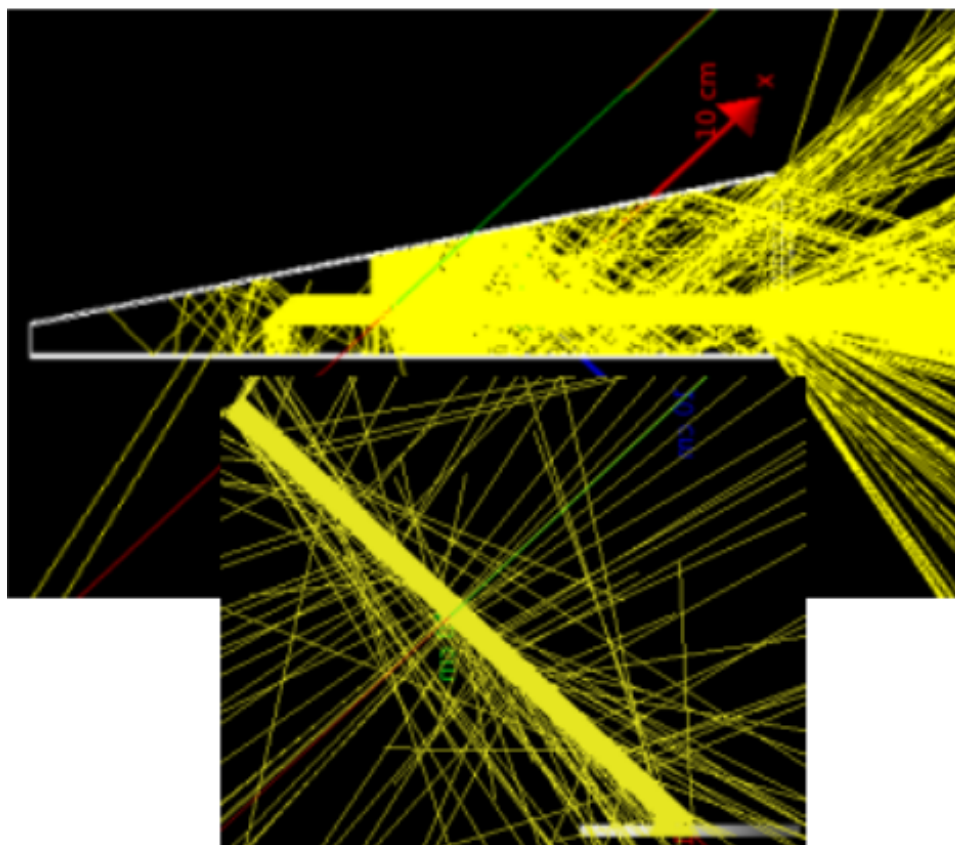
Integrating Detector Design change between PREX-I and PREX-II/CREX

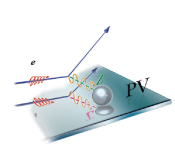
- Orientation between quartz, pmt, and scattered electron changed
 - Allows capture of both sides of Cherenkov cone – instead of losing one side due to critical angle
 - Use TIR inside quartz as light guide – instead of aluminum air-core reflector to direct light to PMT
 - Less sensitivity to extra noise due to delta-ray production
- This change effectively doubles light yield and improves RMS by $\sqrt{2}$
- However, there is more light yield variation for electrons with different incident angles
- ❖ Design validated with G4 optical Monte Carlo benchmarked to “real” Testbeam data



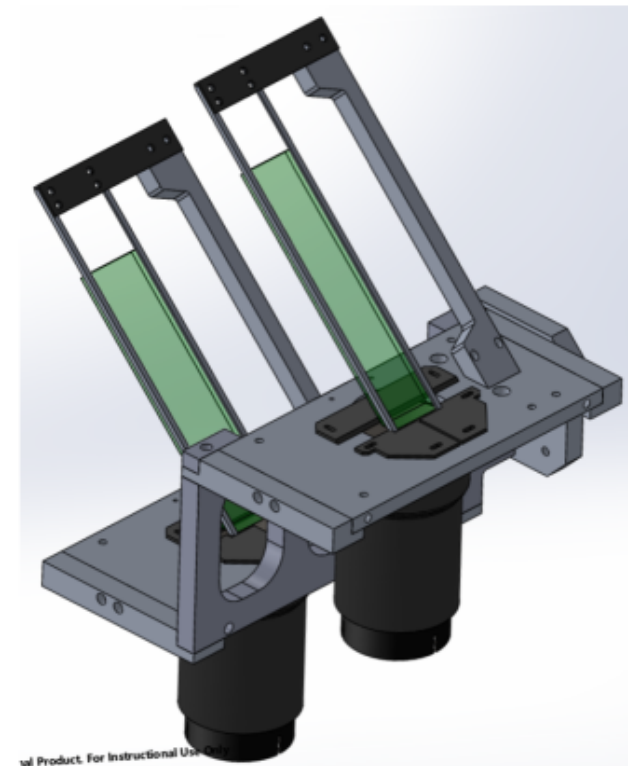
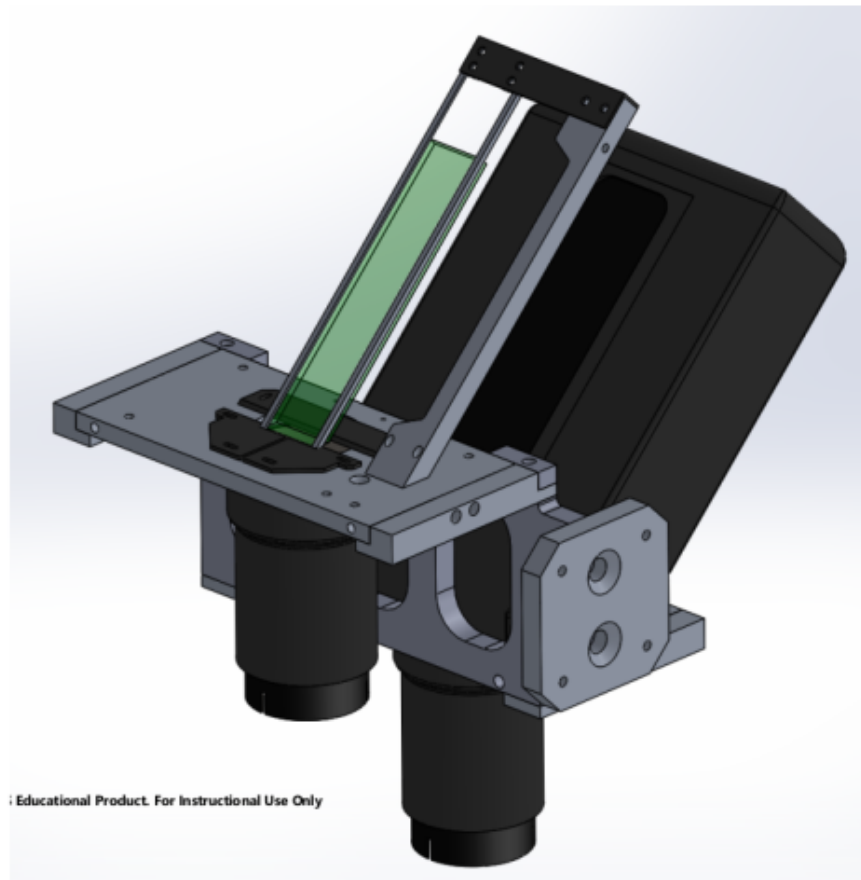
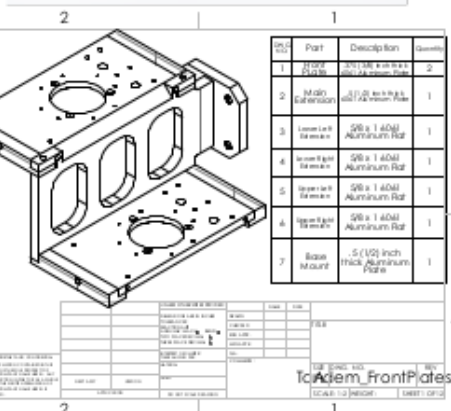
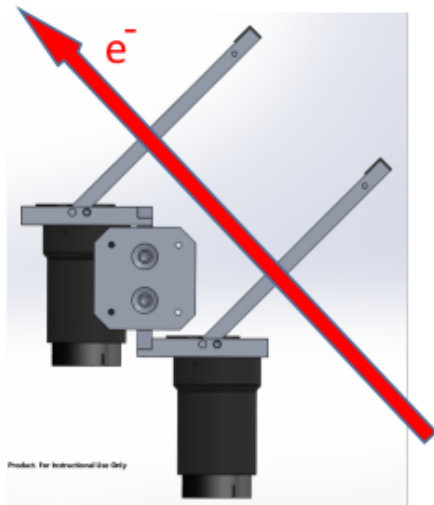


G4 Event Visualizations: PREX-I vs PREX-II/CREX

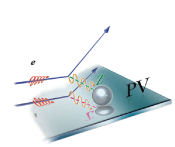




Main Integrating Detectors for PREX-II/CREX

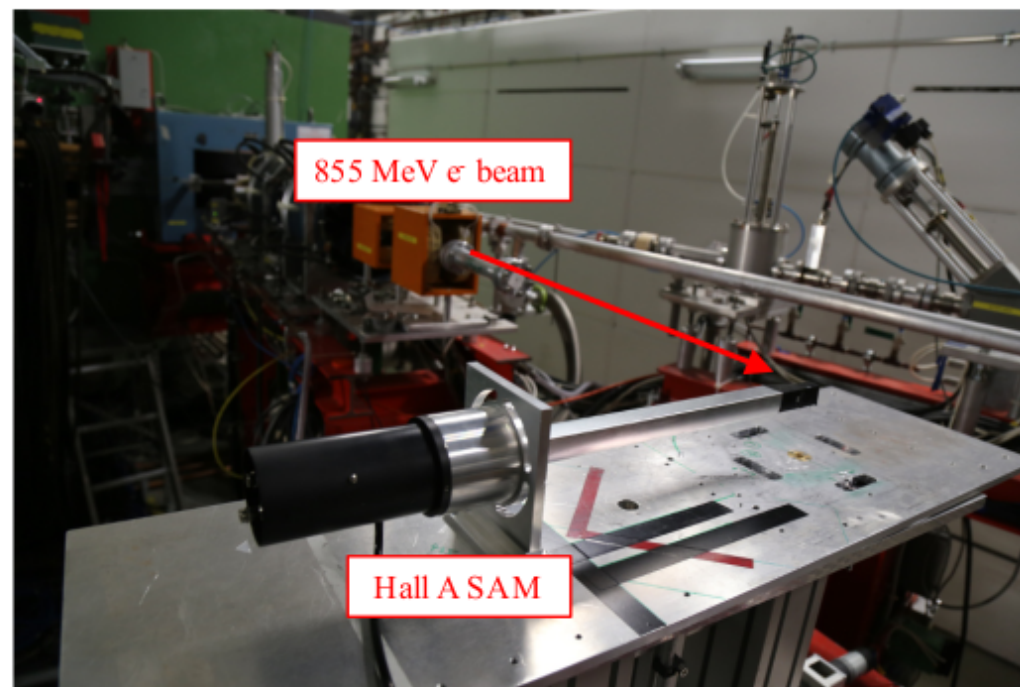
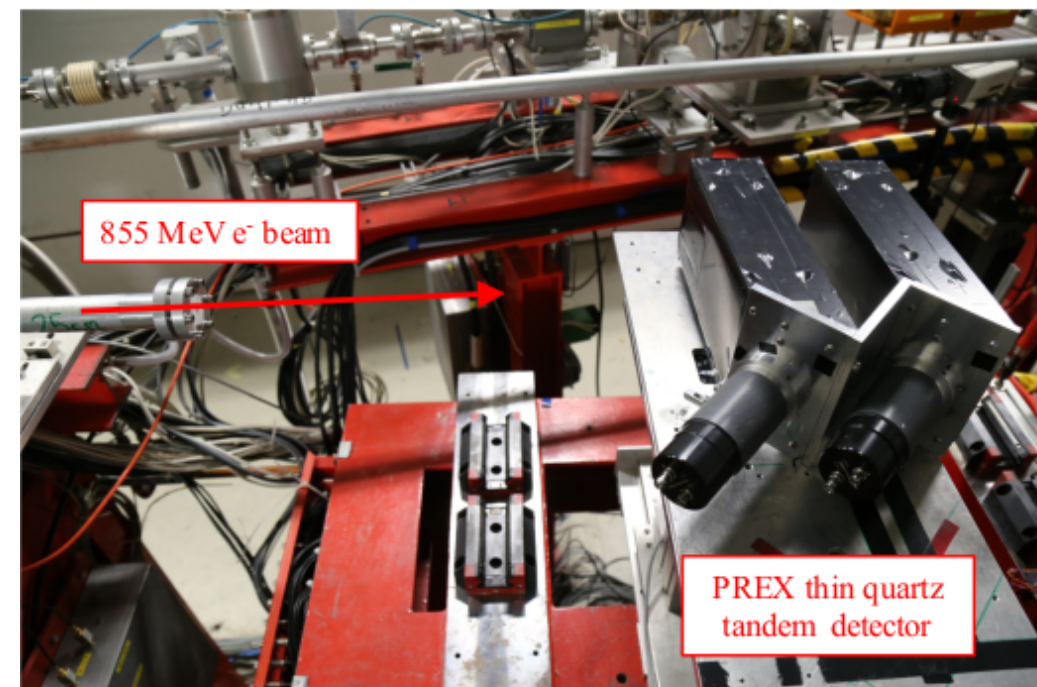


- Both Left and Right HRS main detectors are assembled and ~ready to go
- PREX will use 5 mm thick quartz for all detectors
- CREX will use 6 mm thick quartz upstream and 10 mm downstream



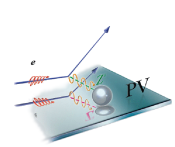
MAMI testbeam May 24-27, 2016

- $\frac{3}{4}$ shift total for PREX-II/CREX and SAM

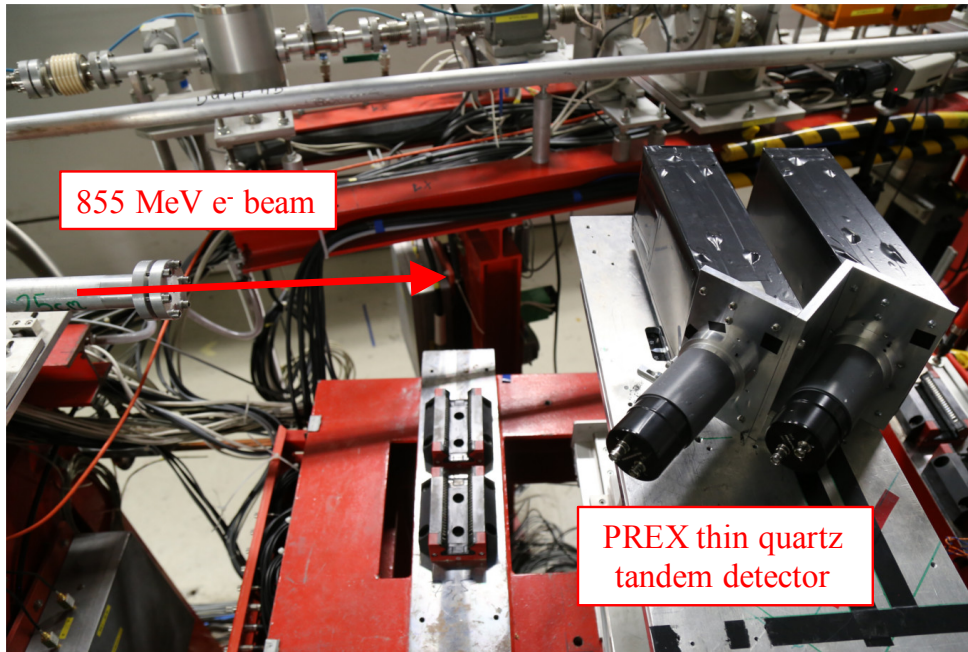


- 6mm and 10mm Tandem mount
- Near normal e^- incidence

- v3 (2015) SAM detector PE yield studies:
 - Miro27 and UVS light-guides
 - With and without 1cm tungsten pre-radiator

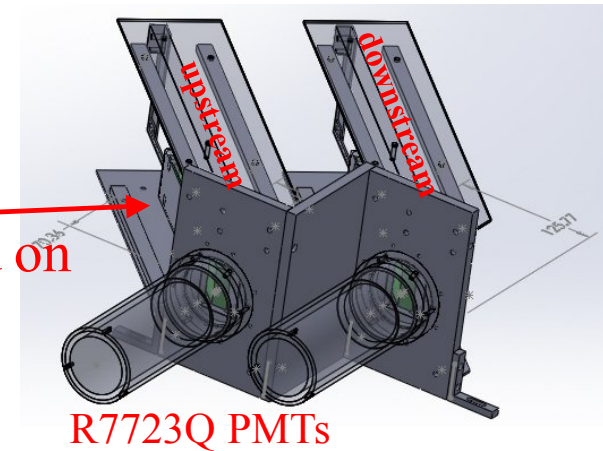


PREX-II/CREX Tandem Detector Tests

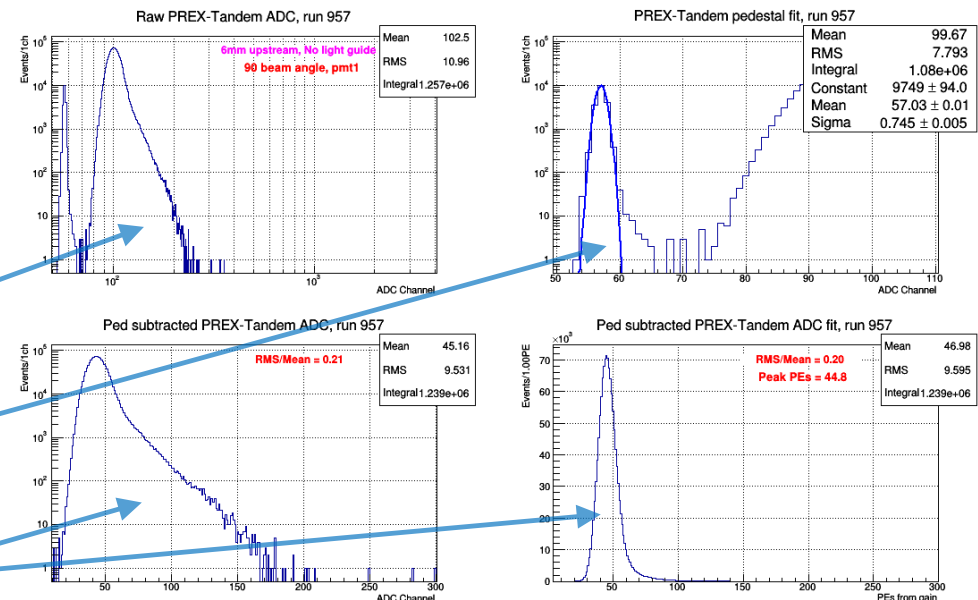


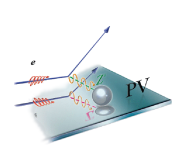
Spectrosil2000 thicknesses: 10mm 6mm and 6mm 10mm

e⁻ beam
Centered on quartz at ~90°

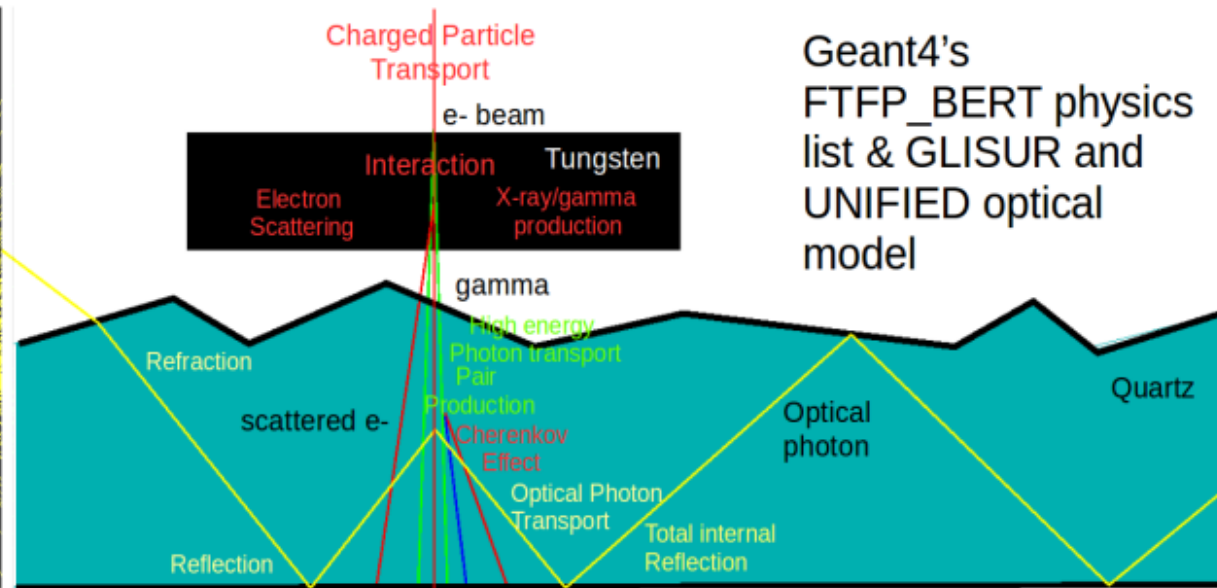
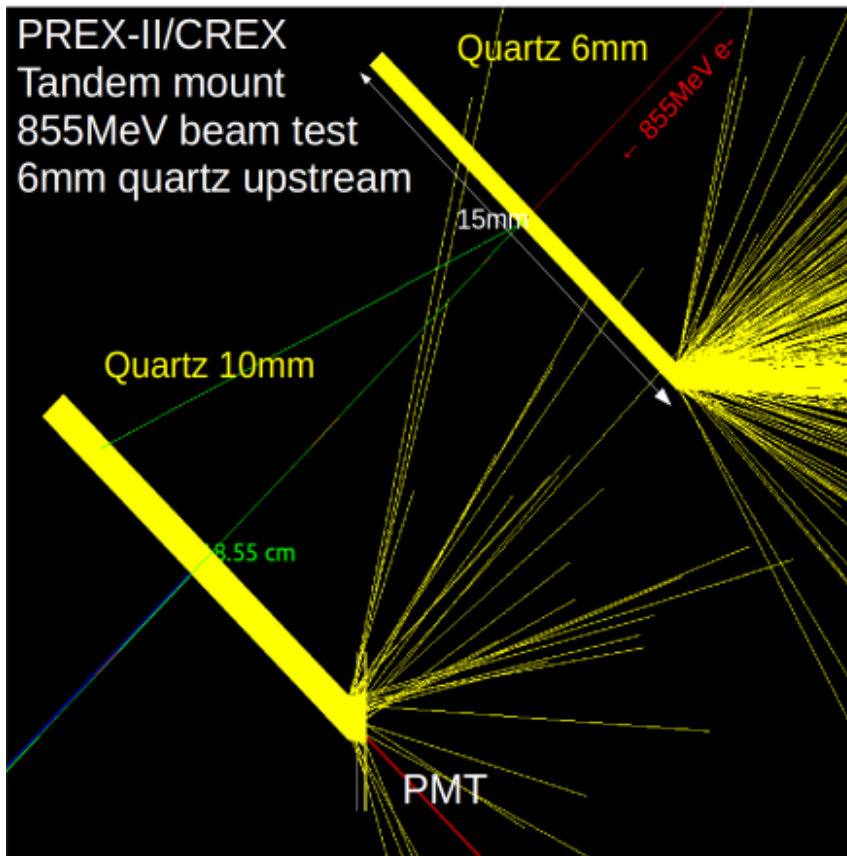


- Quartz spacing same as for rotary tandem mount (~16 cm)
- Used two Hamamatsu R7723Q pmts
- Quartz is wrapped with 1 mil Al. Mylar
- Took runs for each quartz thickness upstream and downstream
- Example raw data, pedestal fit, and ped-corrected ADC and PE dists



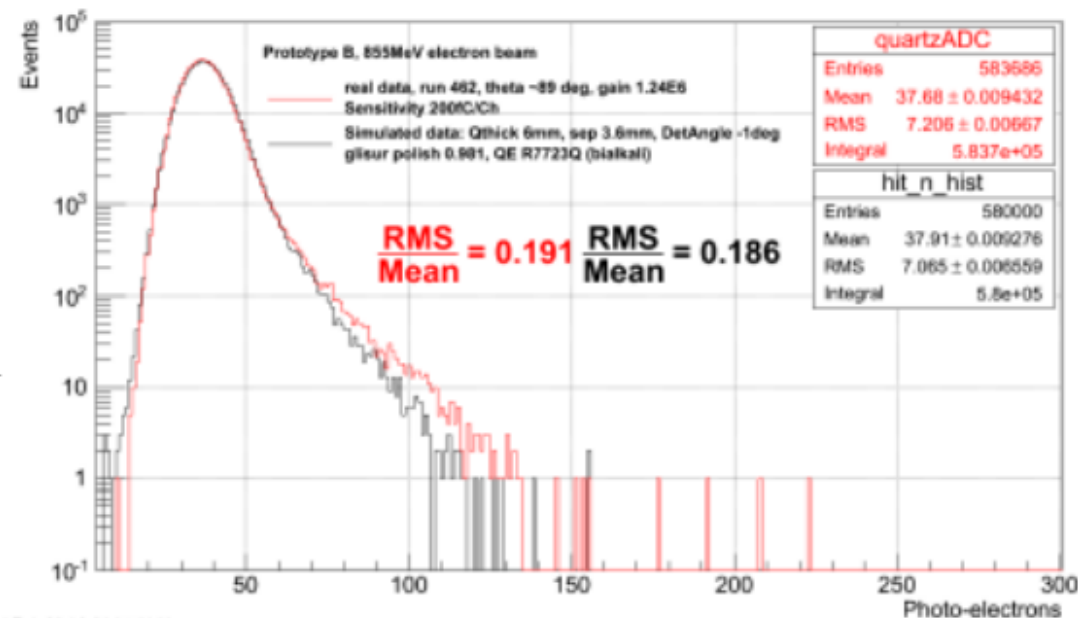


Optical Monte Carlo (qsim) Benchmarking



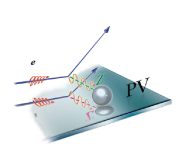
Geant4's FTFP_BERT physics list & GLISUR and UNIFIED optical model

Photo-Electron Distribution - Prototype B Detector



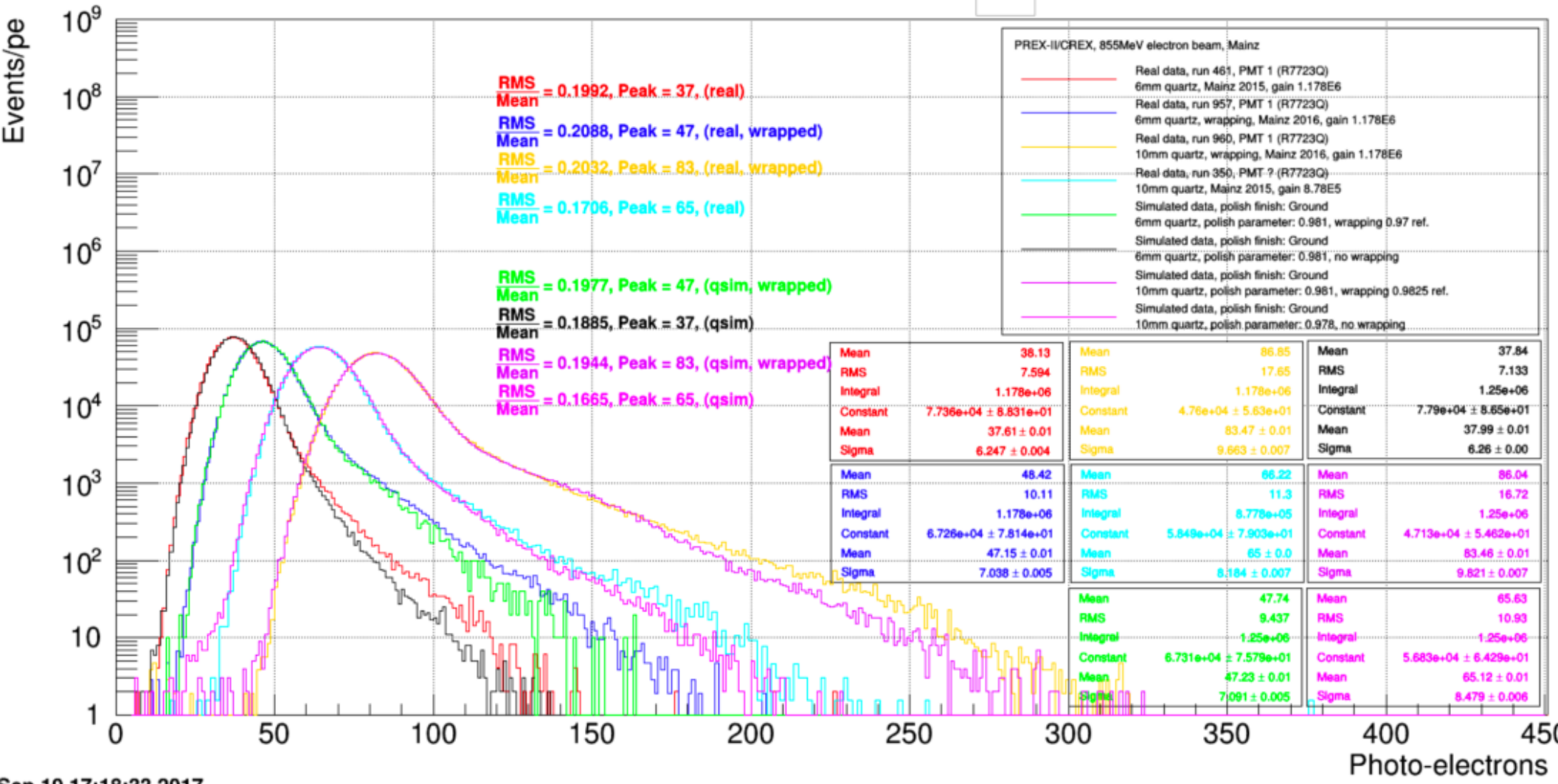
Fri Feb 26 14:44:35 2016

- Detailed geometry; pmt quantum efficiency sampling; refractive index dispersion; light attenuation in quartz; photo-cathode attenuation and reflection; quartz ground polish parameter
- Glisure ground polish parameter is tuned to make agreement between simulation and data

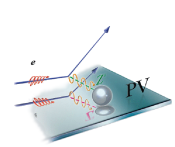


Optical Monte Carlo (qsim) Benchmarking

Photo-Electron Distribution - simulated vs real data

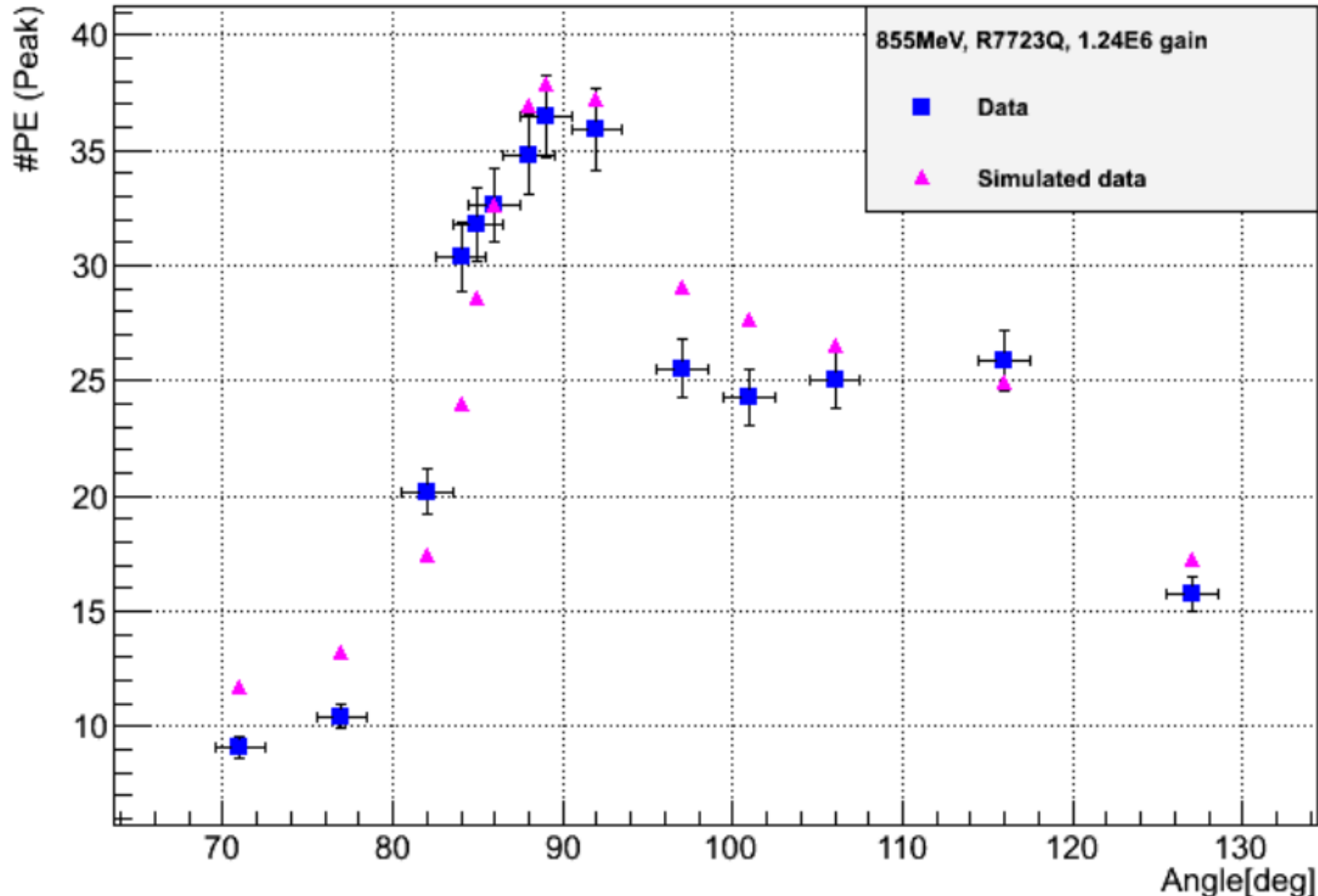


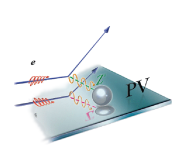
Sep 19 17:18:33 2017



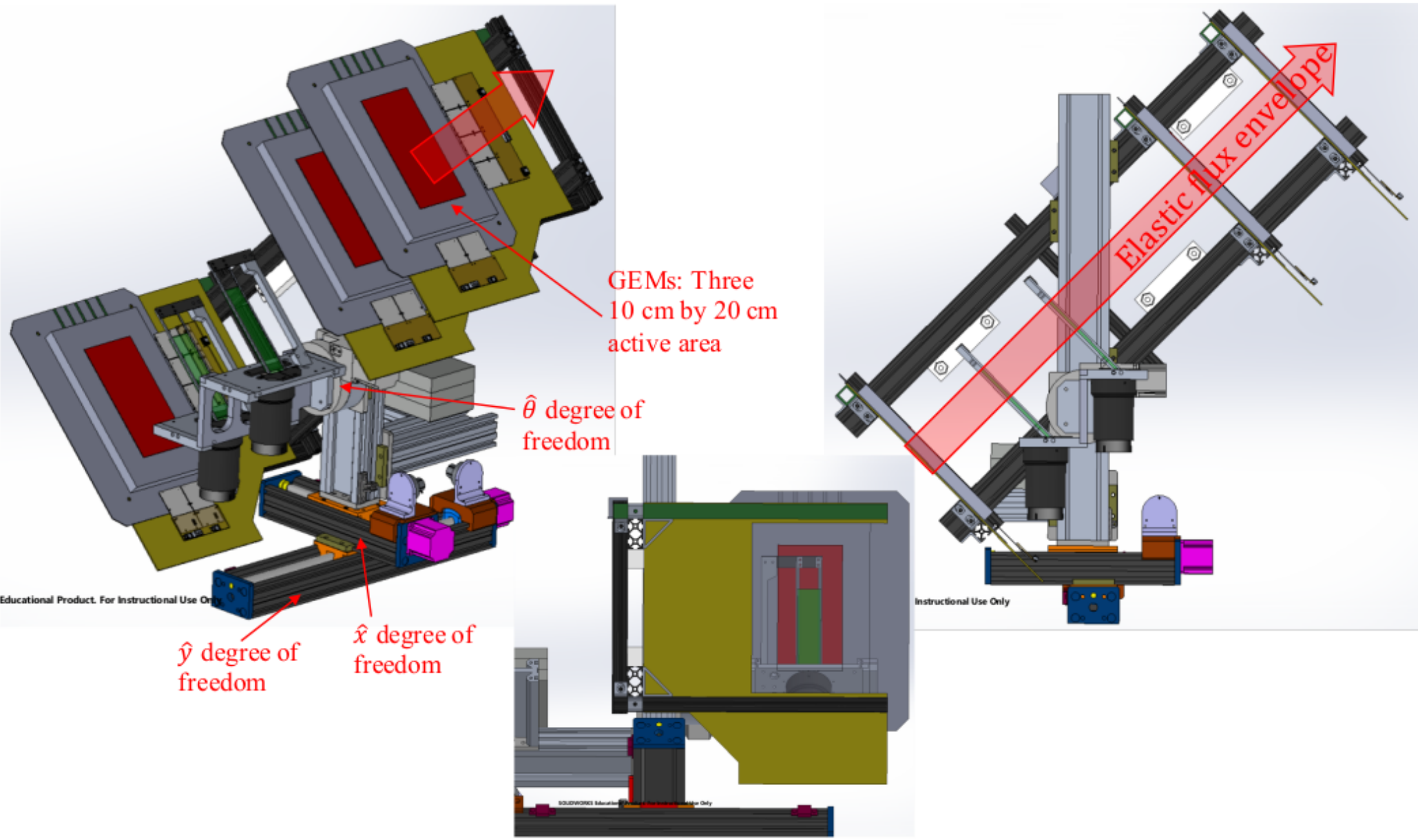
Optical Monte Carlo (qsim) Benchmarking

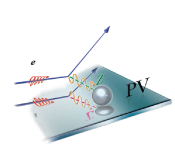
Peak PEs Vs Detector-Beam Angle



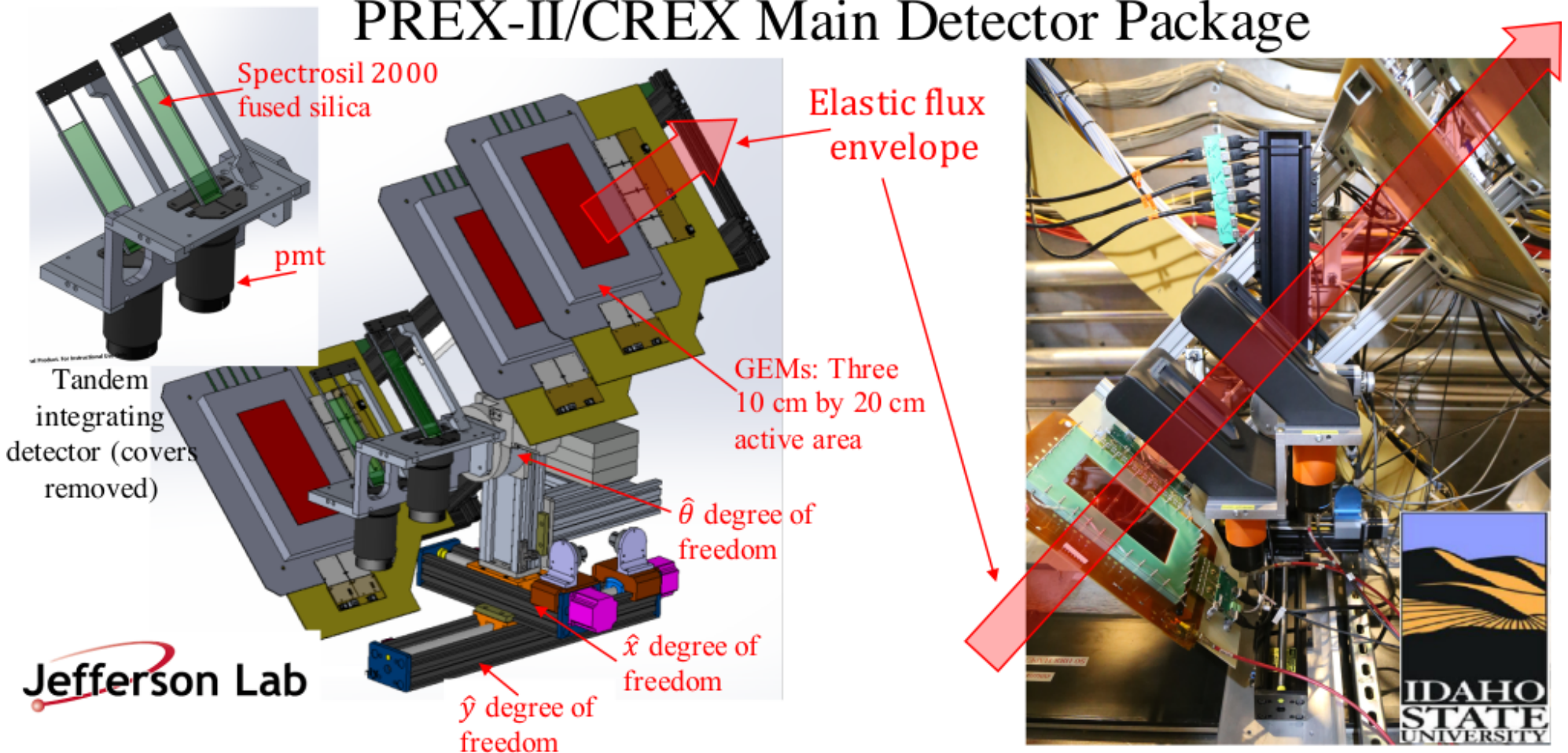


RHRS Tandem PREX-II/CREX Dets with GEMs



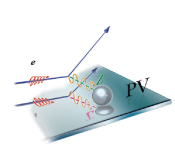


PREX-II/CREX Main Detector Package

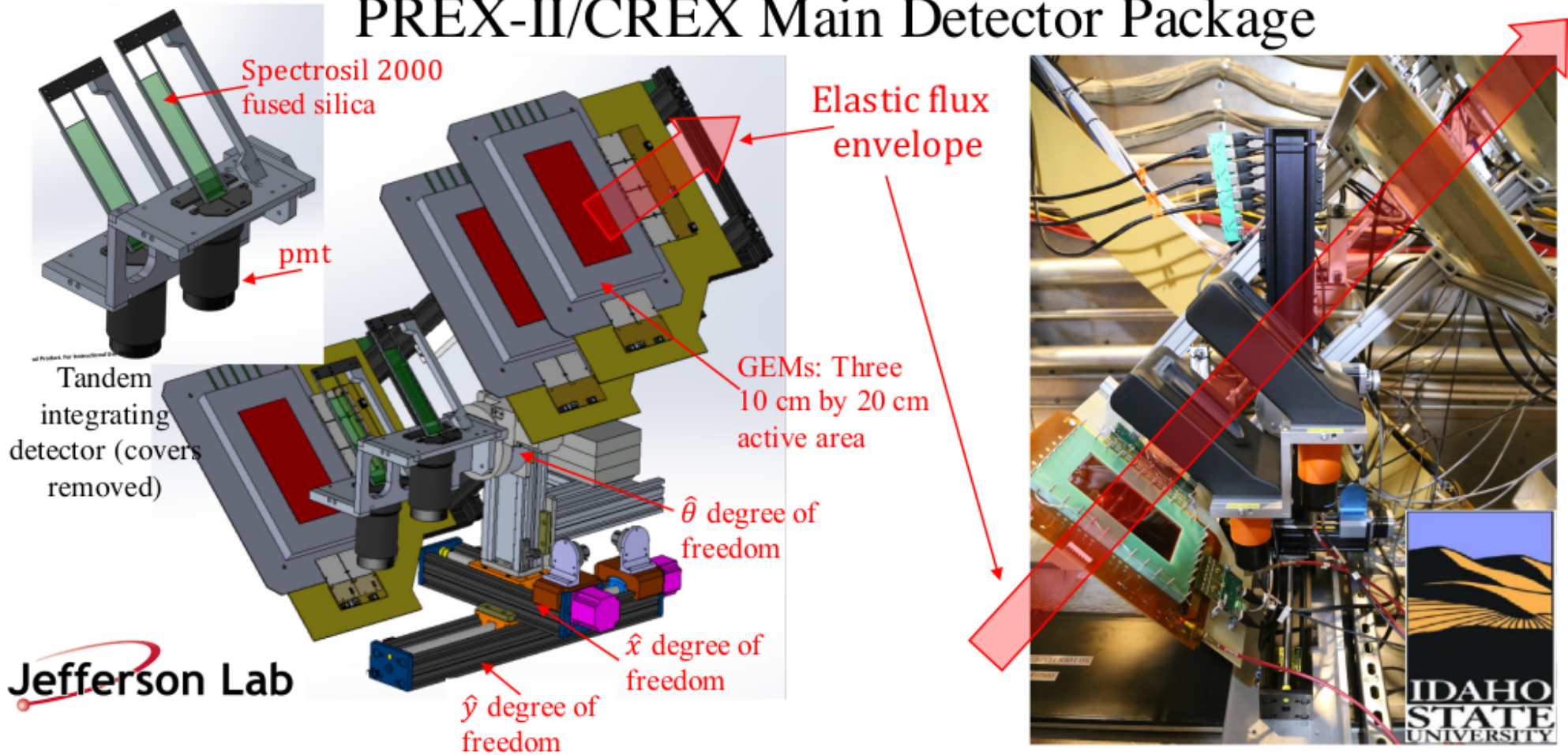


Jefferson Lab

- PREX-II took place over summer 2019 and completed successfully in early September
 - Measured ~ 0.5 ppm A_{PV} from ^{208}Pb with ~ 1 GeV beam at $5^\circ \theta_{\text{lab}}$ to $\sim 3\%$ stat. precision
 - Integrated flux rates were >2 GHz per arm (Left and Right HRS); 26% detector resolution
 - Achieved 14 ppb statistical precision with a few nanometer control on beam positions
 - GEMs operated at 95% efficiency; provided precision Q^2 avg and systematic checks
 - Overall systematic error well below 14 ppb; will extract neutron skin to ± 0.07 fm precision

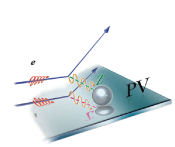


PREX-II/CREX Main Detector Package



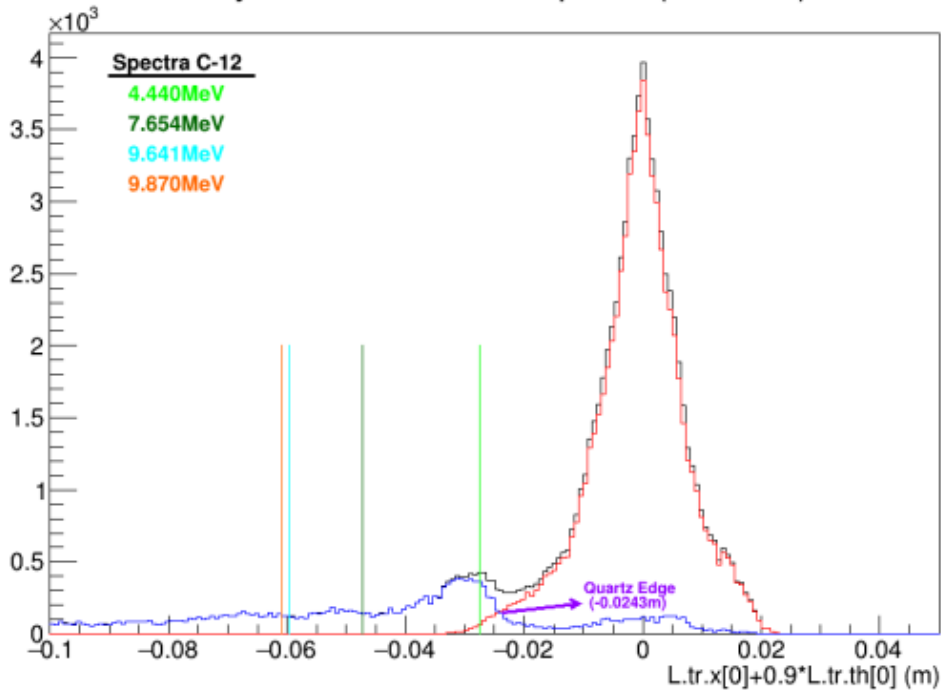
Jefferson Lab

- CREX (Calcium Radius Experiment) will run from this Dec to April 2020 in Hall A, JLab
 - Measure ~ 2 ppm A_{PV} from ^{48}Ca with ~ 2 GeV beam at $5^\circ \theta_{\text{lab}}$ to $\sim 2\%$ stat. precision
 - Integrated flux rates are ~ 30 MHz per arm (Left and Right HRS); 26% detector resolution
 - 45 ppb (proposed) statistical precision with a few nanometer control on beam positions
 - Overall systematic error contribution 26 ppb (proposed); will measure neutron radius and skin with ± 0.02 fm precision



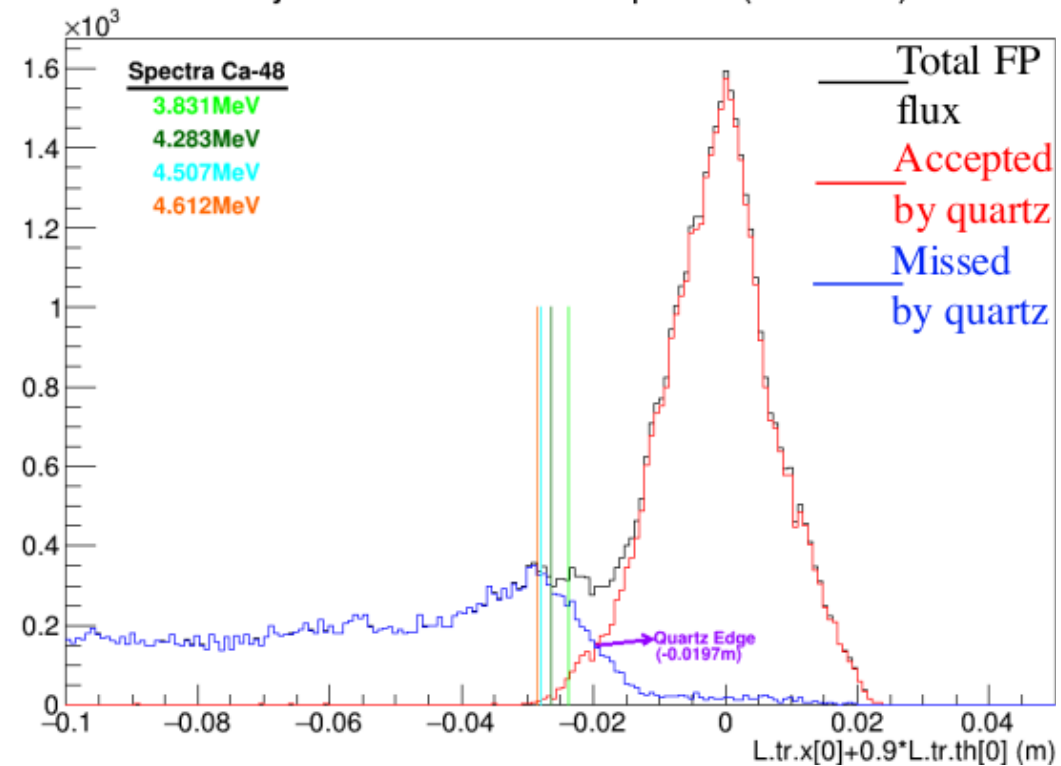
Examples of Focal Plane, Elastic Peak Spectra

Projected x on detector plane (run2652)

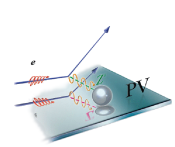


- CREX has established its HRS tune giving expected rates and Q^2 (FOM)

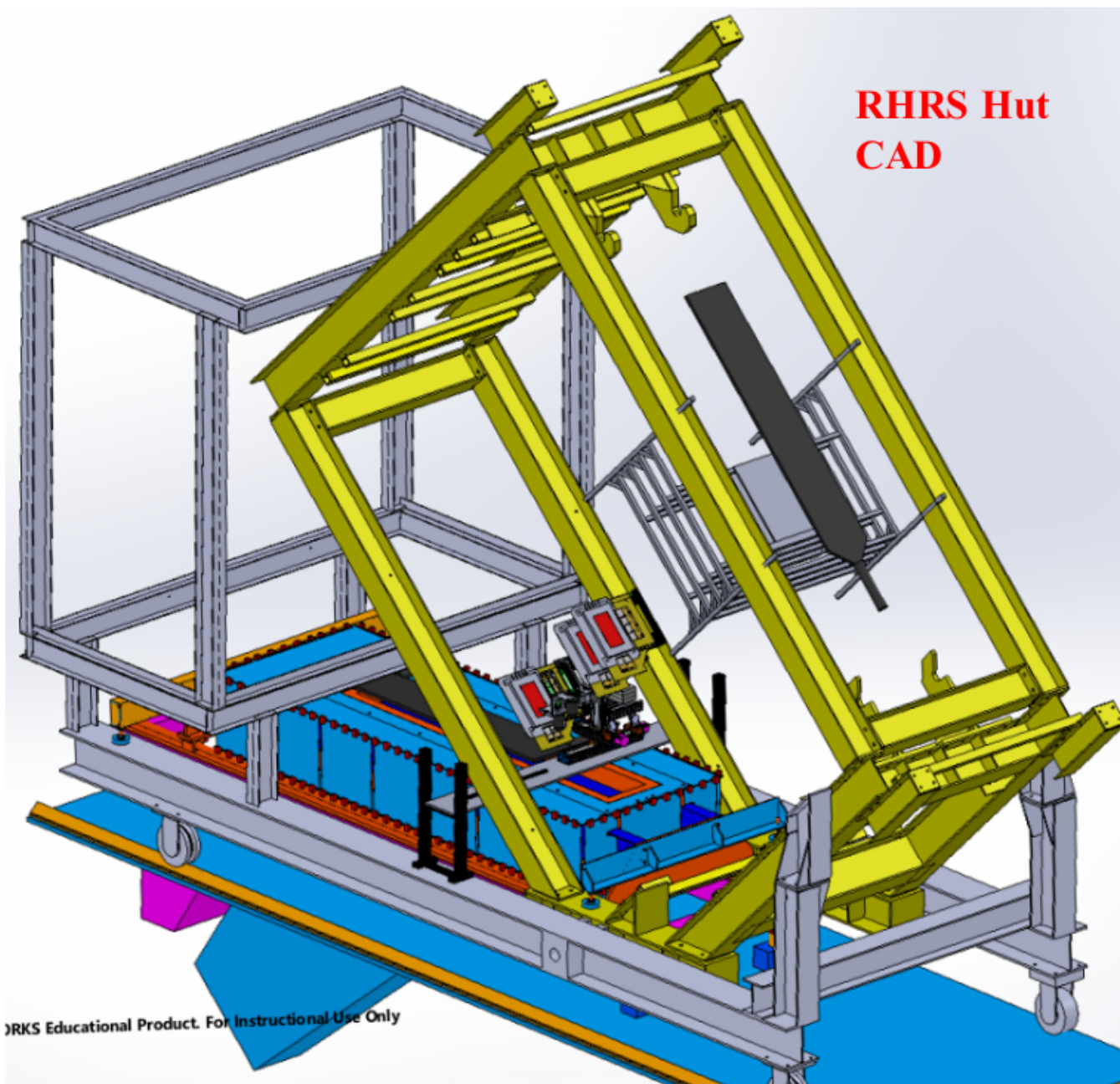
Projected x on detector plane (run2649)

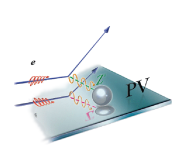


- HRS dispersion: 14.3 cm / % dp/p at det. plane
- At 1-pass (2.183 GeV), this corresponds to ~ 6.57 mm elastic-peak shift per MeV change
- **Energy lock** with full-scale slow drift stability of 0.4 MeV (1.8×10^{-4}) provides ± 1.3 mm stability in peak position

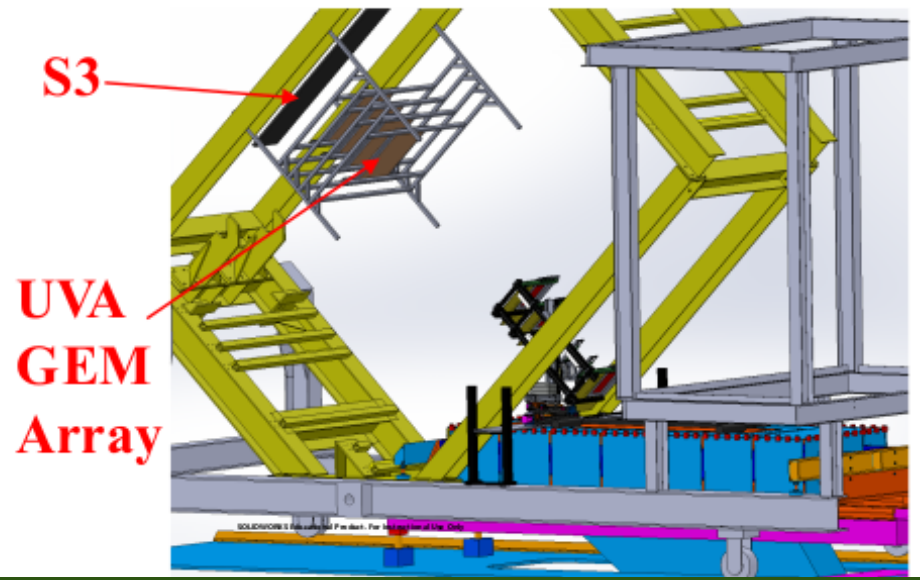
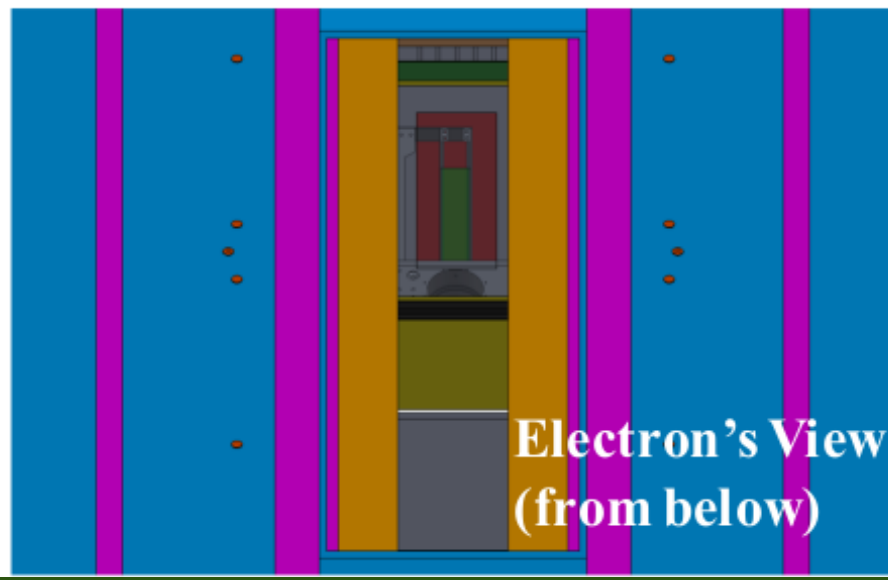
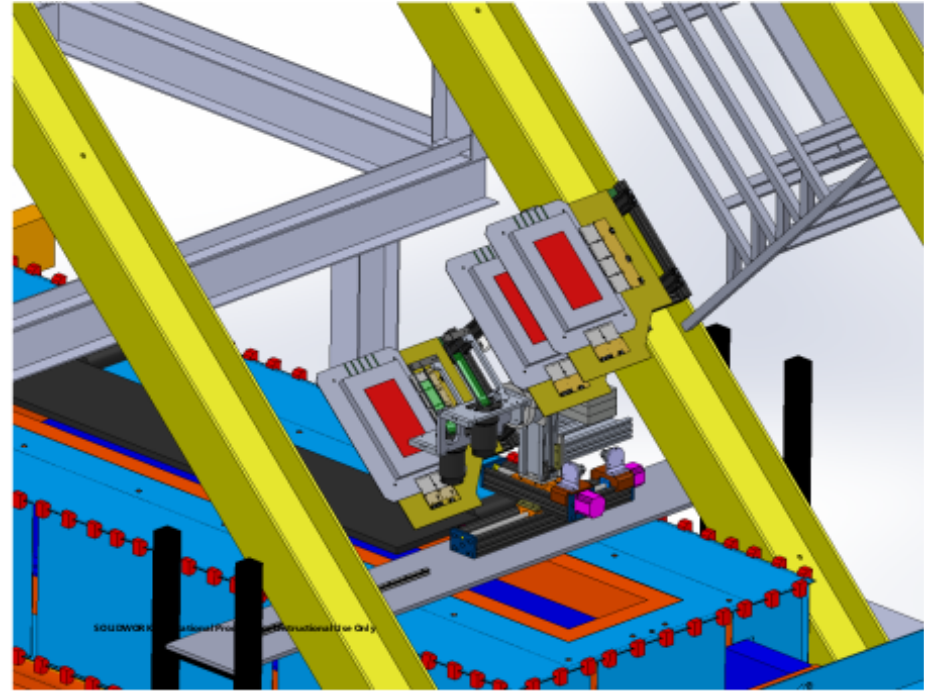
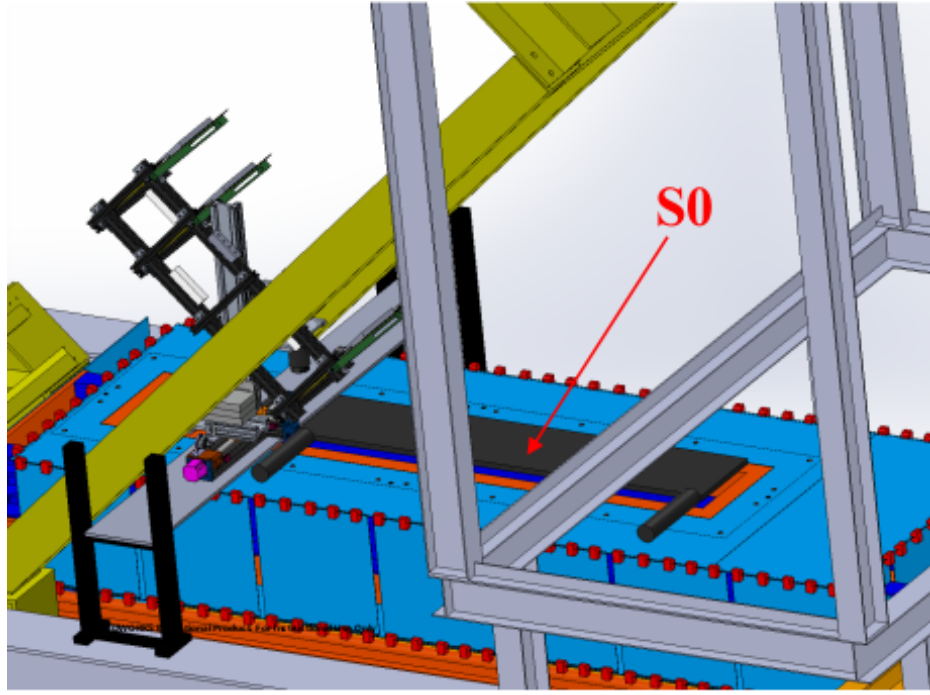


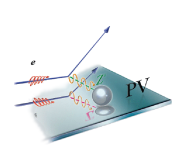
PREX-II/CREX Detector Package



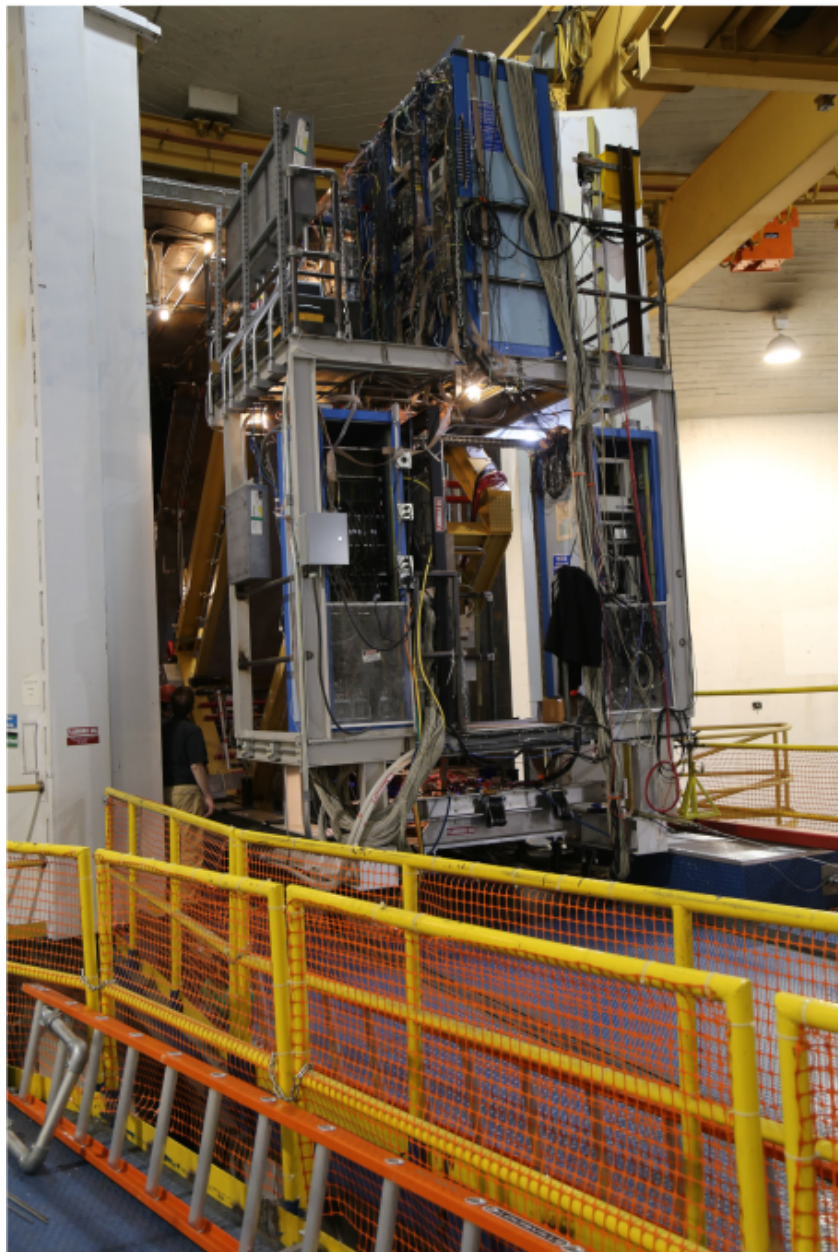


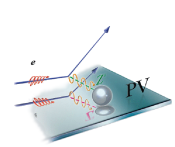
PREX-II/CREX Detector Package



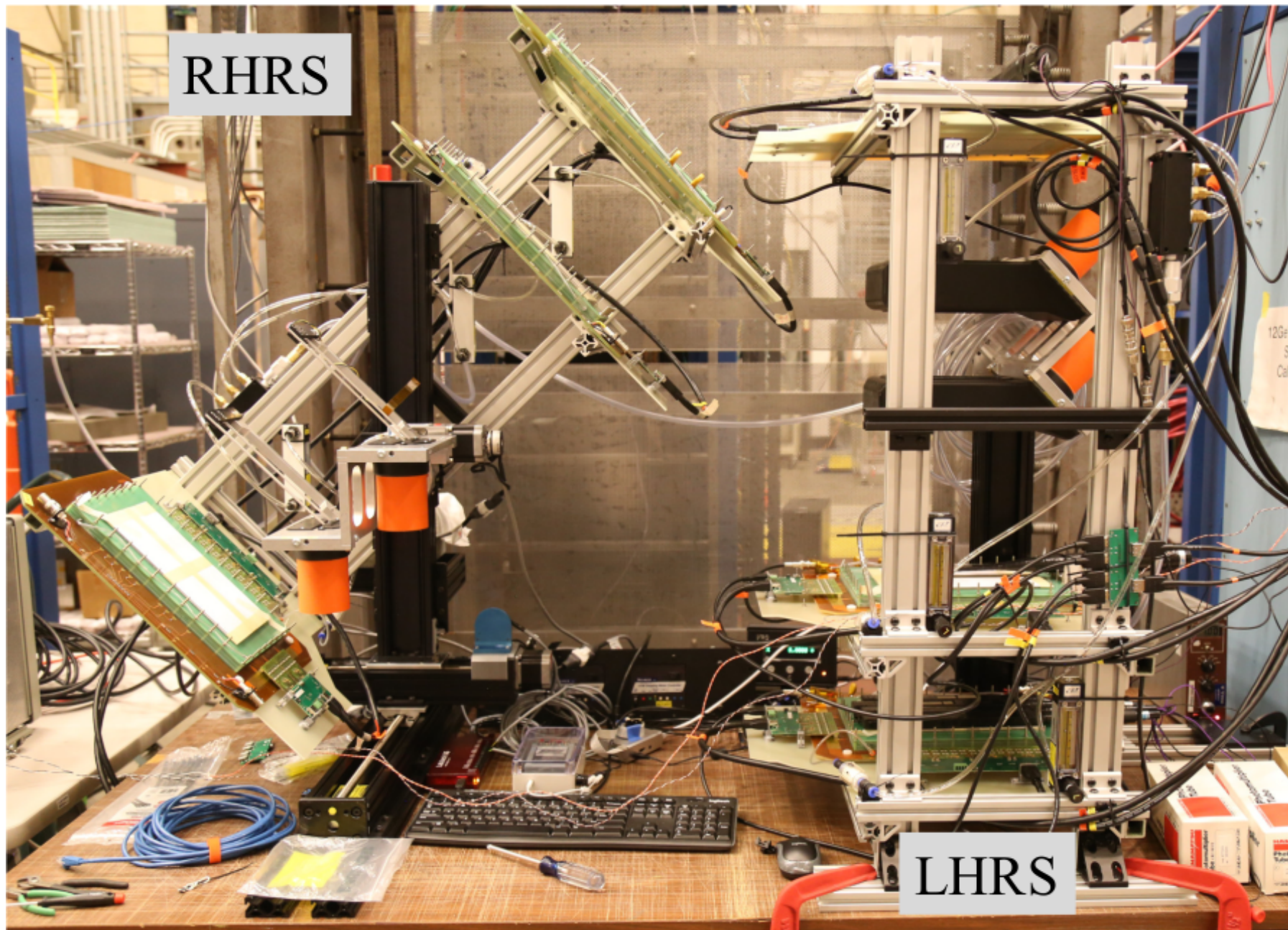


Right HRS Detector Package Installation June 2019



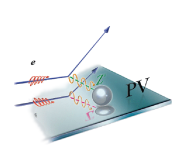


PREX-II/CREX Main Detector Assemblies

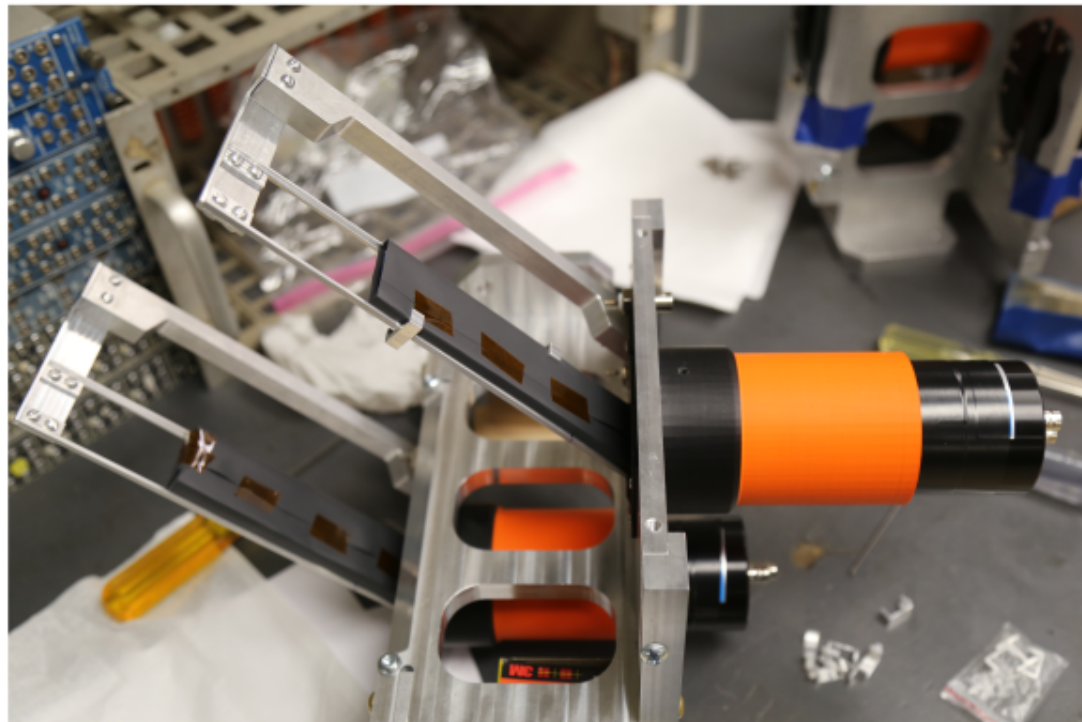
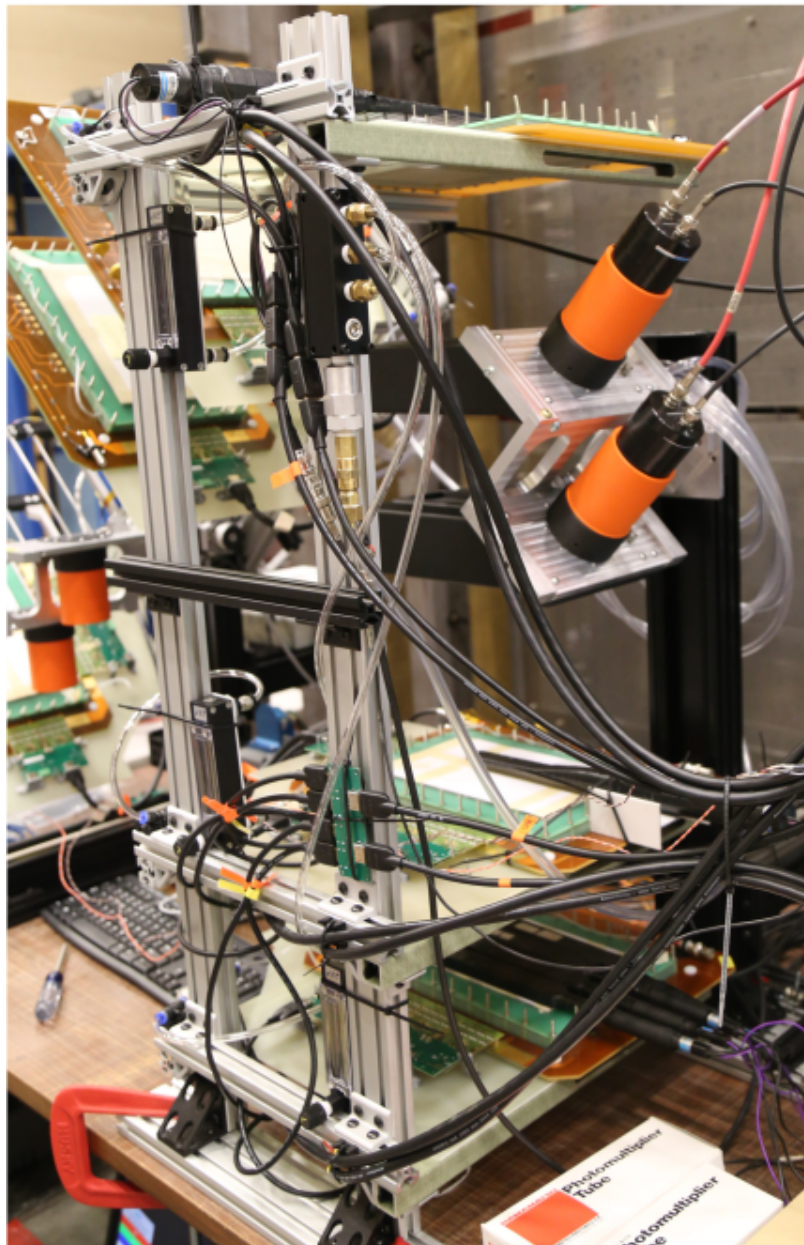


RHRS

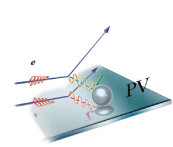
LHRS



LHRS GEM stand in Cosmic-ray mode

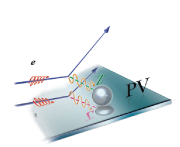


- PREX-II will use 5mm thick quartz.
- Main and A_T detectors will use R7723Q pmts

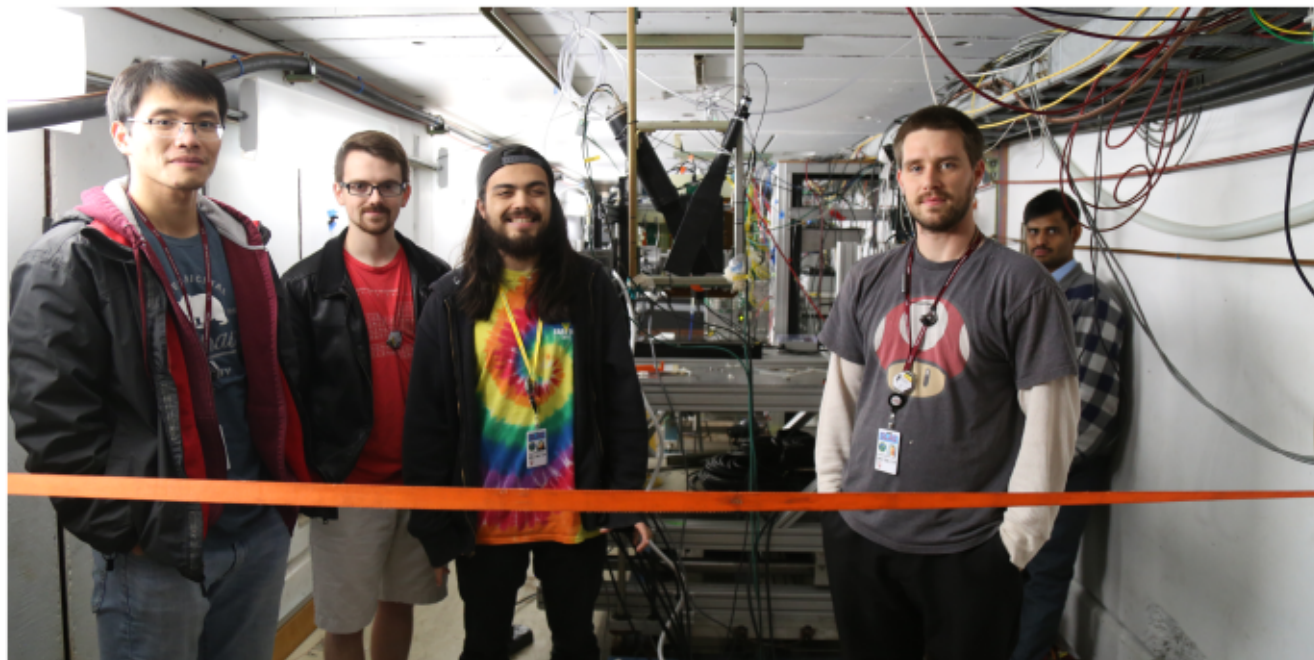
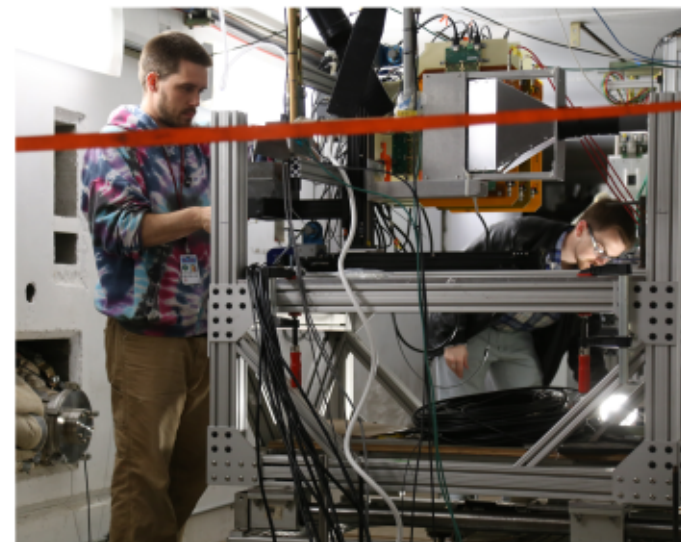


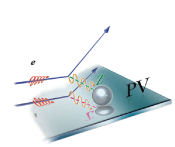
List of past and present undergraduate research assistants within past 6 years

Student	Contribution	Current Status
Kevin Rhine	LG Designs: SAMs and Shwr-max	Grad. 2015
Brady Lowe	DAQ setup, PMT gains, CREX det.	Grad. 2015; MS 2019
Blake French	CODA event-viewer, Cosmic-stand	Grad. 2015; job at Micron
Dayah Chrisman	PMT gain analysis macro	Grad. 2015; Grad.Stud. MSU
Will Gorman	Cosmic-ray data analysis	Grad. 2014; Grad.Stud. U of Roch.
Max Sturgeon	Bending Al. Light Guides for SAMs	Grad. 2017
Chase Juneau	CAD; reflectivity meas.	Grad. 2017; job at INL
Daniel Sluder	Shower-max support frame CAD, ...	Grad. 2016; MS 2018
Joey McCullough	GEM readout backplanes; SLAC tests	Grad. 2017; MS expected 2019
C. Royal Cole	SLAC testbeam stand	Grad. Dec 2018; Medical School
Eighdi Aung	GEM CAD	Grad. 2019; Grad. Stud. Va Tech
Rajul Chauhan	PREX-II/CREX det. motion control	Grad. 2019
Justin Gahley	SLAC testbeam stand motion control	Expected Grad. 2020
Alec Lepisto	3D printing parts; SLAC analysis	Expected Grad. 2021
Brandon Pearson	Designing and 3D printing parts	Expected Grad. 2021



Students at Work at Jefferson Lab and SLAC





Summary and Future Plans

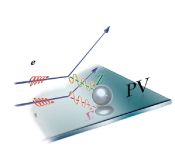
- PVES is a precision tool for measuring weak-charge distributions with implications for nuclear structure and BSM discovery

PREX/CREX:

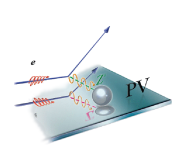
- PREX-II collected 80% of proposed data and together with PREX-I will reach full precision: ± 0.07 fm resolution on the neutron radius and skin of ^{208}Pb with implications for neutron stars, ...
- CREX currently running and on target to reach proposed measurement goal: ± 0.02 fm resolution on the neutron radius and skin of ^{48}Ca with implications for nuclear structure and forces

Integrating Detectors

- Much progress over past 5 years – new robust design
- "thin" quartz detectors becoming well understood
- Future detector work for MOLLER will quantify rad-hardness of detector materials, including quartz and aluminum reflectors

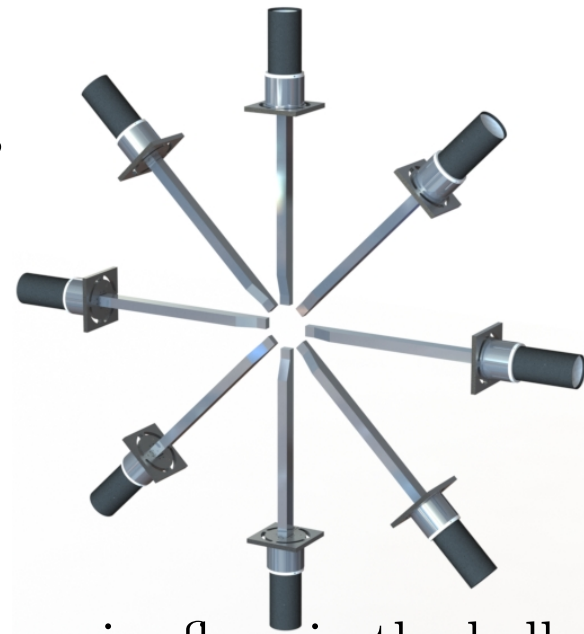


Extra Slides

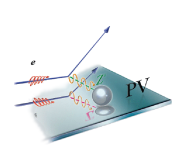


Motivations for Downstream Lumi's or SAM's

- Need them for their high sensitivity to helicity-correlated beam parameters
 - Detect charged particle flux at extreme forward angles
 - Very high rates and thus narrow pulse-pair widths – powerful diagnostic tool

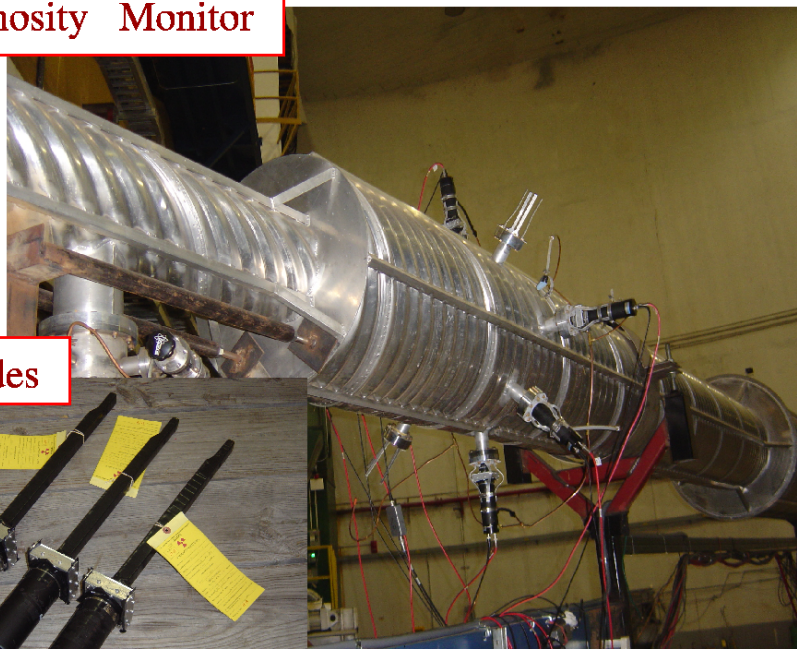


- Provides measure of overall electronic noise floor in the hall
- In theory, should have very low/no PV asymmetry and can serve as null asymmetry monitor
- Symmetric 8 piece design helps disentangle beam position and angle HCBP's while 8 SAM sum is insensitive
- Could provide important tests of regression procedures

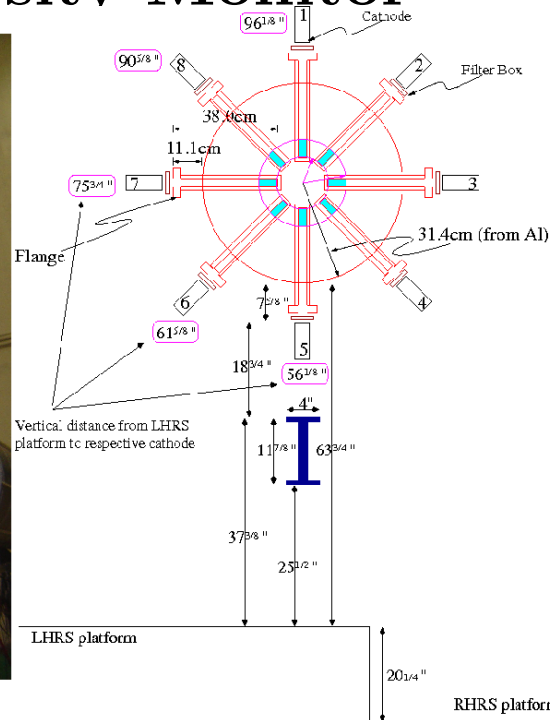


Old Hall A Luminosity Monitor

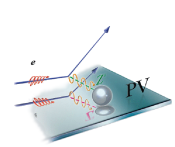
Luminosity Monitor



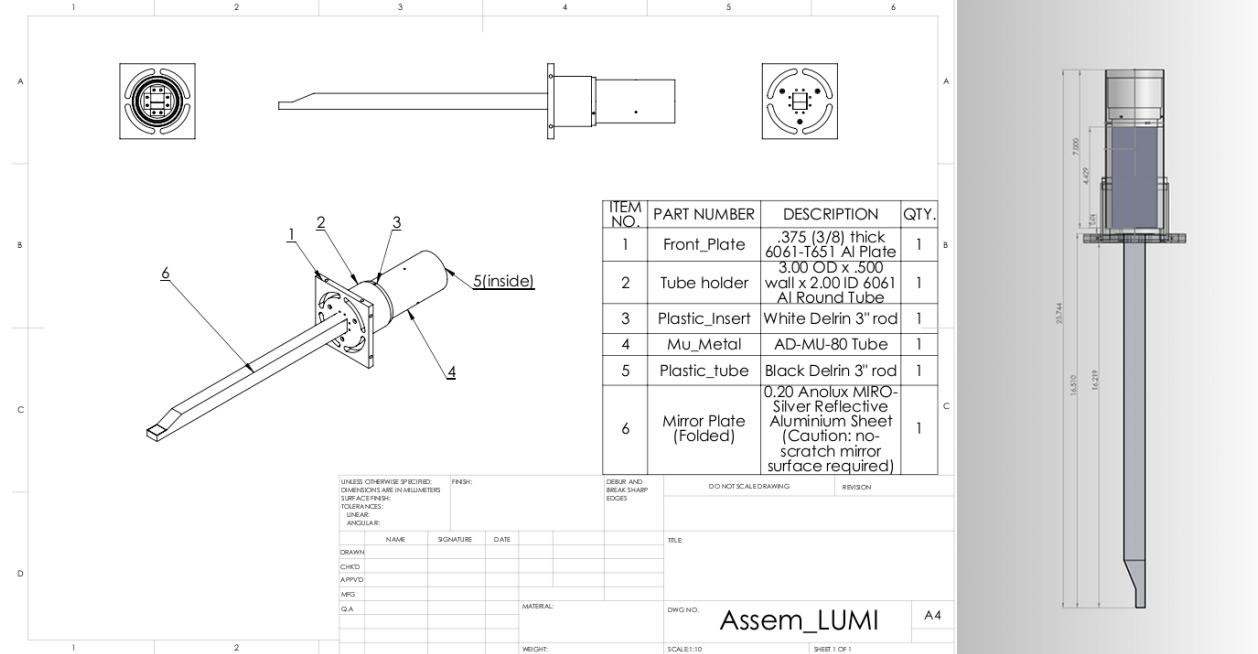
Upgrades



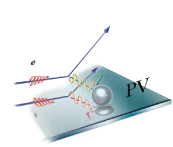
- Conceptual Design 2002–Riad Suleiman; refurbished in 2008
- 8 quartz Cherenkov detectors with air-core light guides placed symmetrically around beam line 7m downstream of pivot
- Used $6.0 \times 2.0 \times 1.0 \text{ cm}^3$ quartz placed 4.5 cm from beam center \Rightarrow 0.3 - 0.8 deg polar angle acceptance



Luminosity Monitor Re-design (SAMs)



- Incorporate Qweak's downstream Lumi experience:
 - Use pre-radiator and "unity gain" PMT
 - Use radially smaller, but thicker quartz
 - May achieve desired linearity at anticipated photocathode currents, but running unity gain mode guarantees it
 - Use TRIUMF preAmps at SAM for signal cond. and gain
- *Work within constraints of existing beampipe insertion tubes*

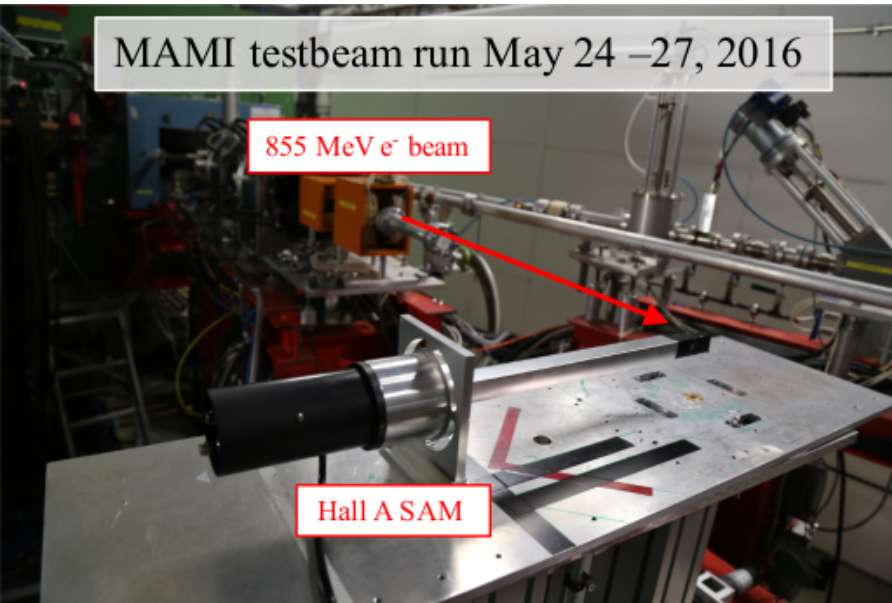


Final SAM Design and 2016 Testbeam

MAMI testbeam run May 24 -27, 2016

855 MeV e⁻ beam

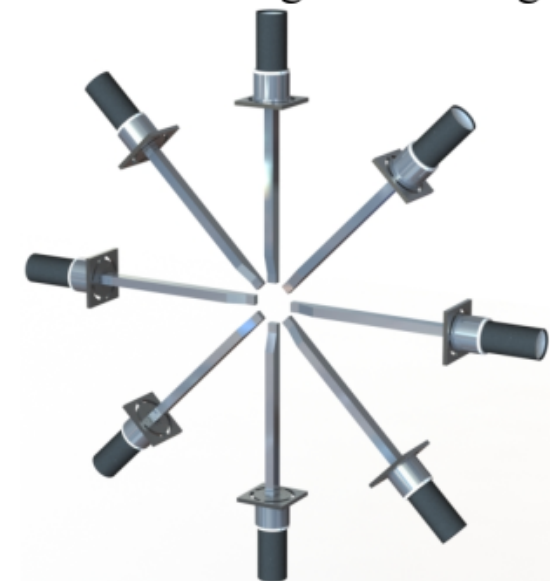
Hall A SAM



- Final (v3) SAM detector PE yield studies:
 - MiroSilver27 and UVS light-guides
 - With and without 1cm tungsten pre-radiator



Small Ange Monitors:
Detect ~0.5° target scattering

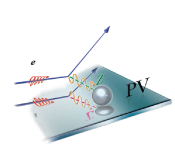


Assembled & Installed in Hall A Fall 2015



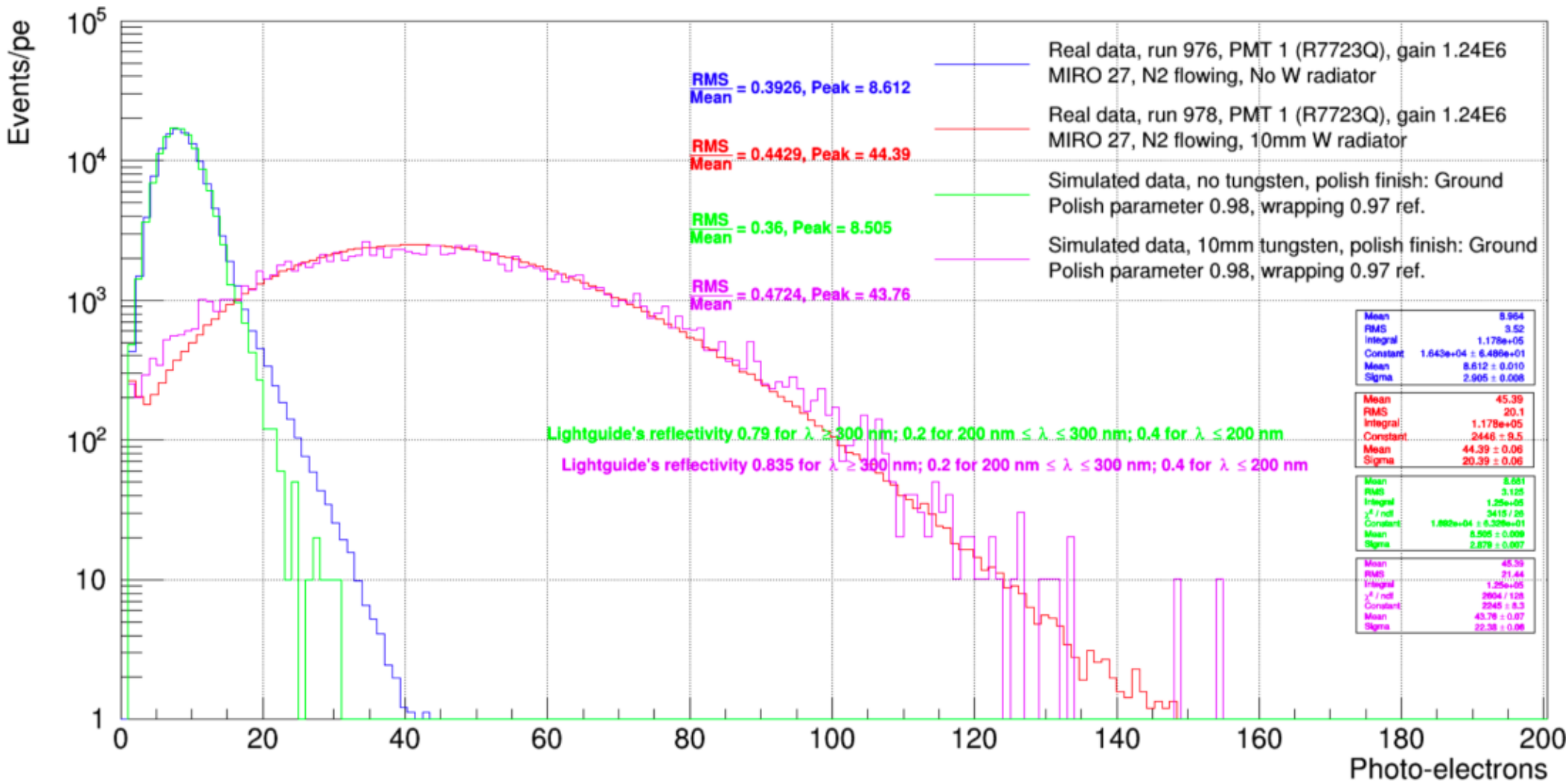
v3 SAM detector

- Quartz: 33 x 20 x 13 mm³
- Miro27 LG: 36 x 2.6 x 2.1 cm³
- Optimized 1-bounce funnel mirror
- Unity or high-gain R375 2" PMTs
- Use of pre-radiator not decided
- Dry-air inlet and outlet ports
- Custom flange adapter for easy de-install/re-install (radcon permitting)

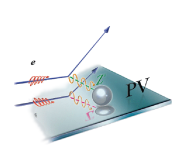


Optical Monte Carlo (qsim) Benchmarking: SAMs

Photo-Electron Distribution - simulated vs real data

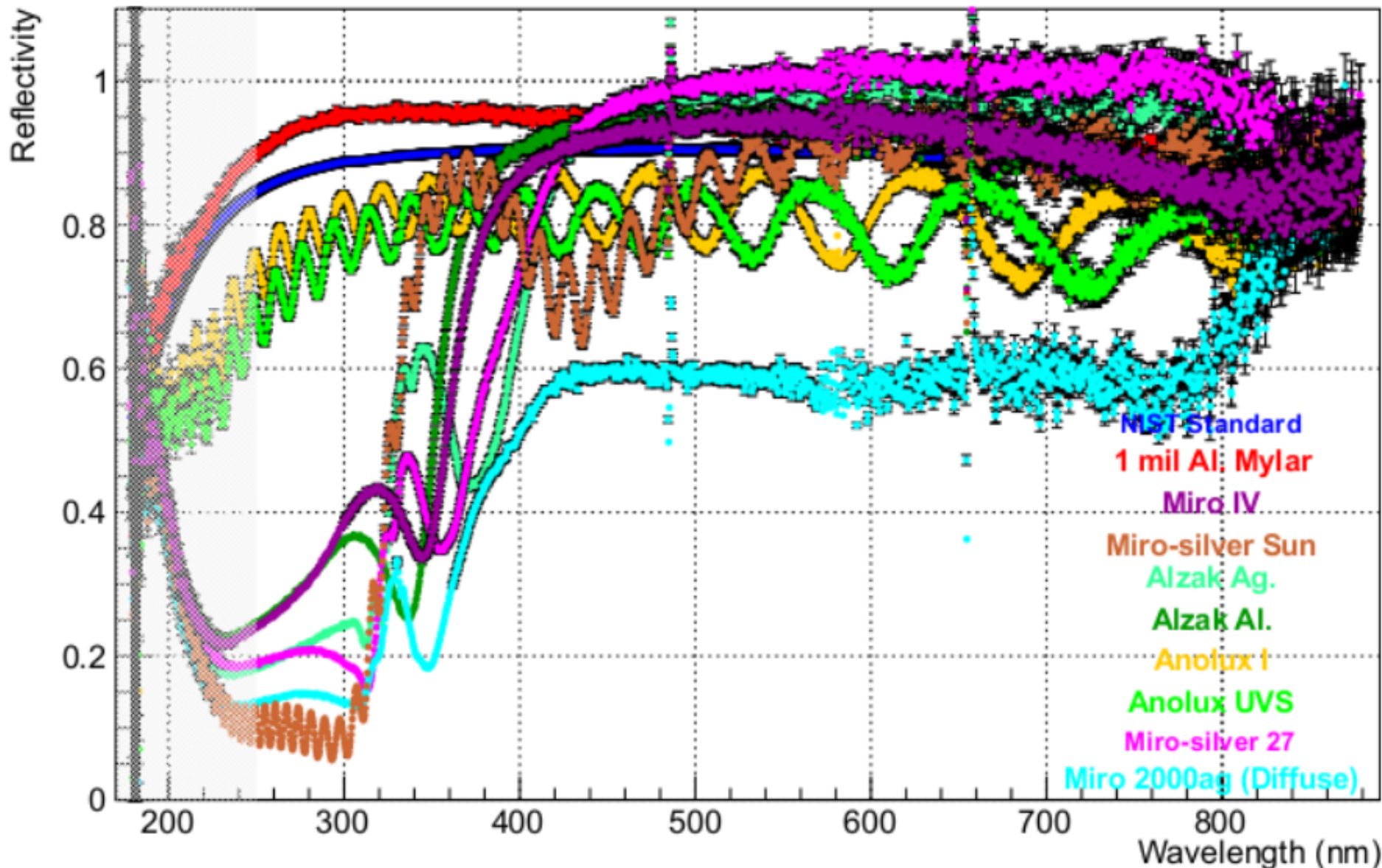


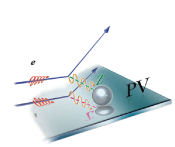
Sep 25 01:24:10 2017



SAM light guide reflectivity: explored many options

Reflectivity (~90 degree)





The MOLLER Project at Jefferson Lab:

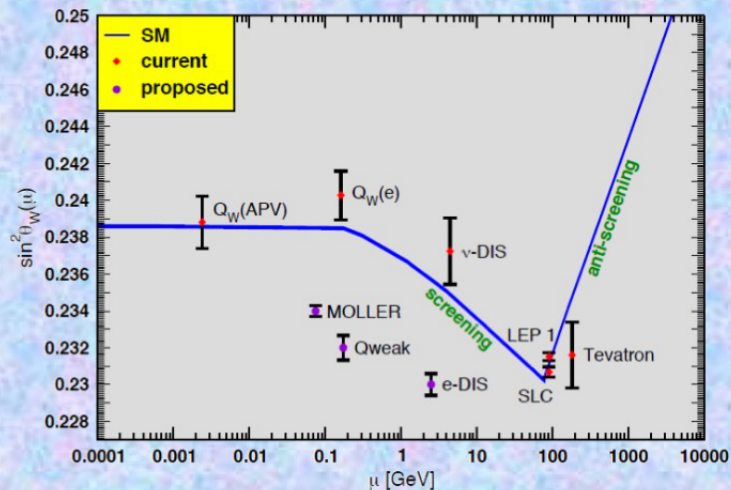
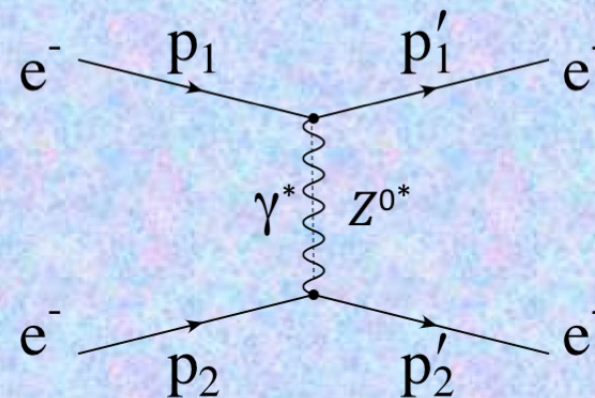
Measurement of

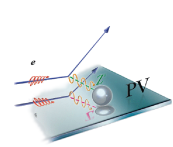
Lepton

Lepton

Electroweak

Reaction



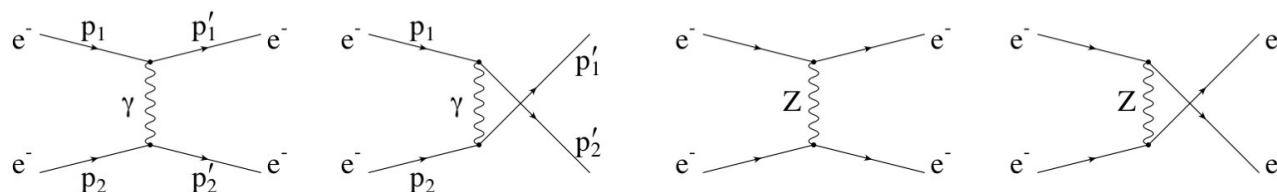


Møller Scattering A_{PV} Measurement

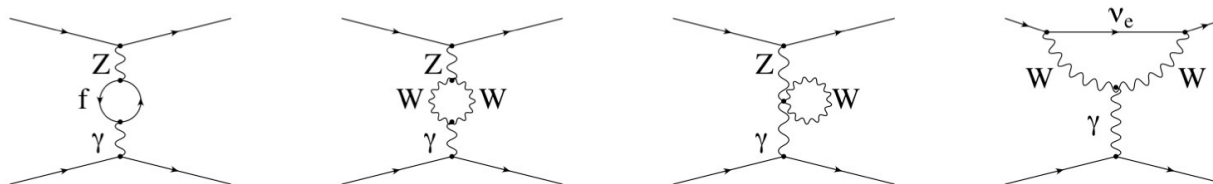
- MOLLER aimed at precision measurement of parity-violating asymmetry A_{PV} in polarized electron-electron scattering.
- Standard Model gives precise prediction for Møller A_{PV} –which can be measured as a test.

$$A_{PV} = \frac{\sigma_R - \sigma_L}{\sigma_R + \sigma_L} = \frac{M_\gamma M_Z}{M_\gamma^2} = m_e E_{lab} \frac{G_F}{\sqrt{2}\pi\alpha} \frac{4\sin^2\theta_{lab}}{(3 + \cos^2\theta_{lab})^2} Q_W^e,$$

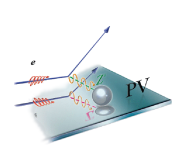
$$Q_W^e \equiv 4 \cdot g_V^e \cdot g_A^e = -(1 - 4\sin^2\theta_W) \tag{1}$$



Feynman diagrams for Moller Scattering at tree level



γ - Z mixing diagrams and W loops. “Hard” radiative corrections involving the massive vector bosons—modify the tree level prediction significantly.

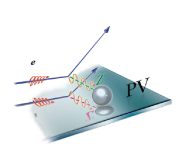


The MOLLER A_{PV} Measurement

- At proposed kinematics: $11\text{GeV } e_{\text{beam}}^-$ ($75\mu\text{A}$, $80\% P_e$), and $5\text{mrad} < \theta_{lab} < 20\text{mrad}$:
→ Predicted $\langle A_{PV} \rangle = 36\text{ppb}$ at $\langle Q^2 \rangle = 0.0056 (\text{GeV}/c)^2$
- For 49 (PAC) week run: $\delta A_{PV} = 0.74\text{ppb}$:
→ $\delta Q_W^e / Q_W^e = \pm 2.1\%(\text{stat}) \pm 1.0\%(\text{syst})$
→ $\delta \theta_W = \pm 0.00026(\text{stat}) \pm 0.00012(\text{syst}) \sim 0.1\%$ precision!

Challenging 4th generation measurement requiring:

- Unprecedented precision matching of electron beam characteristics for Left versus Right helicity states
- Precision non-invasive, redundant continuous beam polarimetry
- Precision knowledge of luminosity, spectrometer acceptance (Q^2) and backgrounds



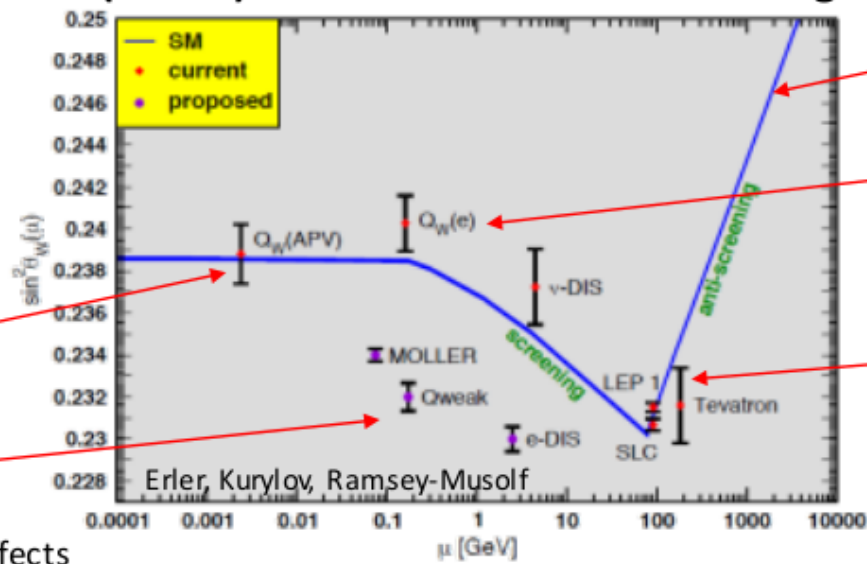
MOLLER Motivations

Ultra-precise (~0.1%) measurement of weak mixing angle will test SM

Running of $\sin^2\theta_W$: complicated and scheme-dependent – many orders in loops of all particles

6s → 7s ¹³³Cs atomic transition

Major improvements for near future

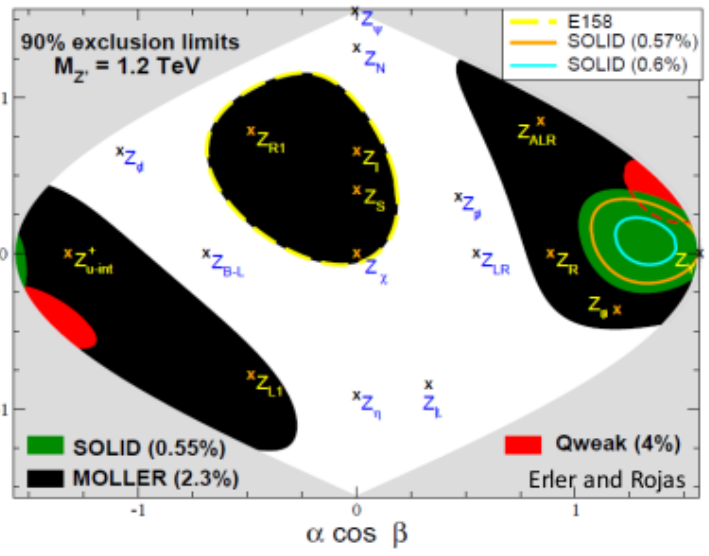
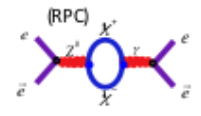
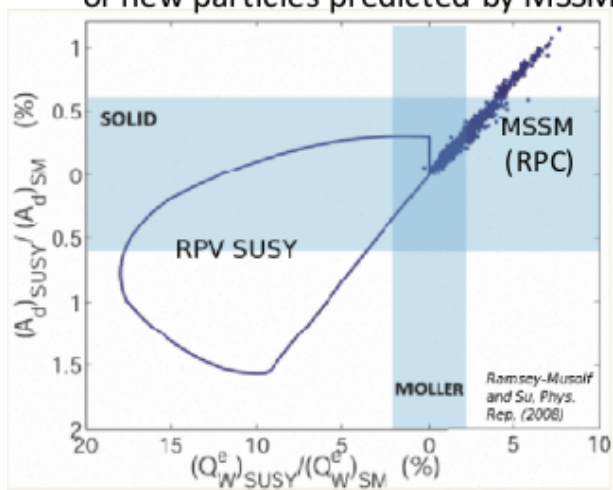


Electroweak fit with uncertainty

Parity violating Moller scattering (E158)

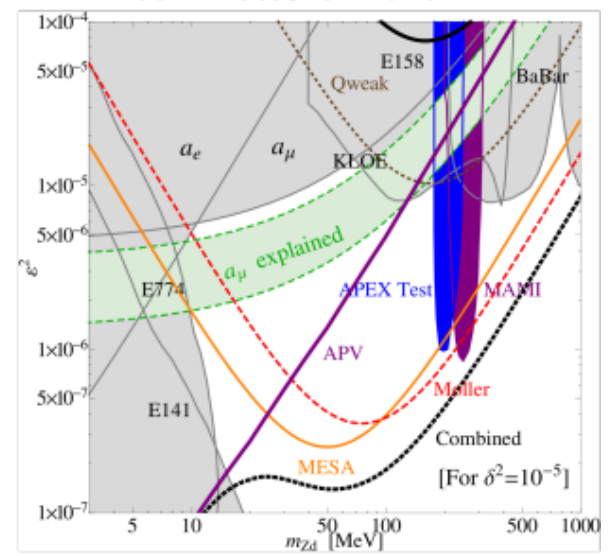
Collider experiments near Z-pole (most precise 0.1%)

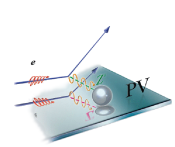
❖ Sensitivity to radiative loop effects of new particles predicted by MSSM



❖ MOLLER can help discriminate between competing GUT models which predict new 1 – 2 TeV Z's

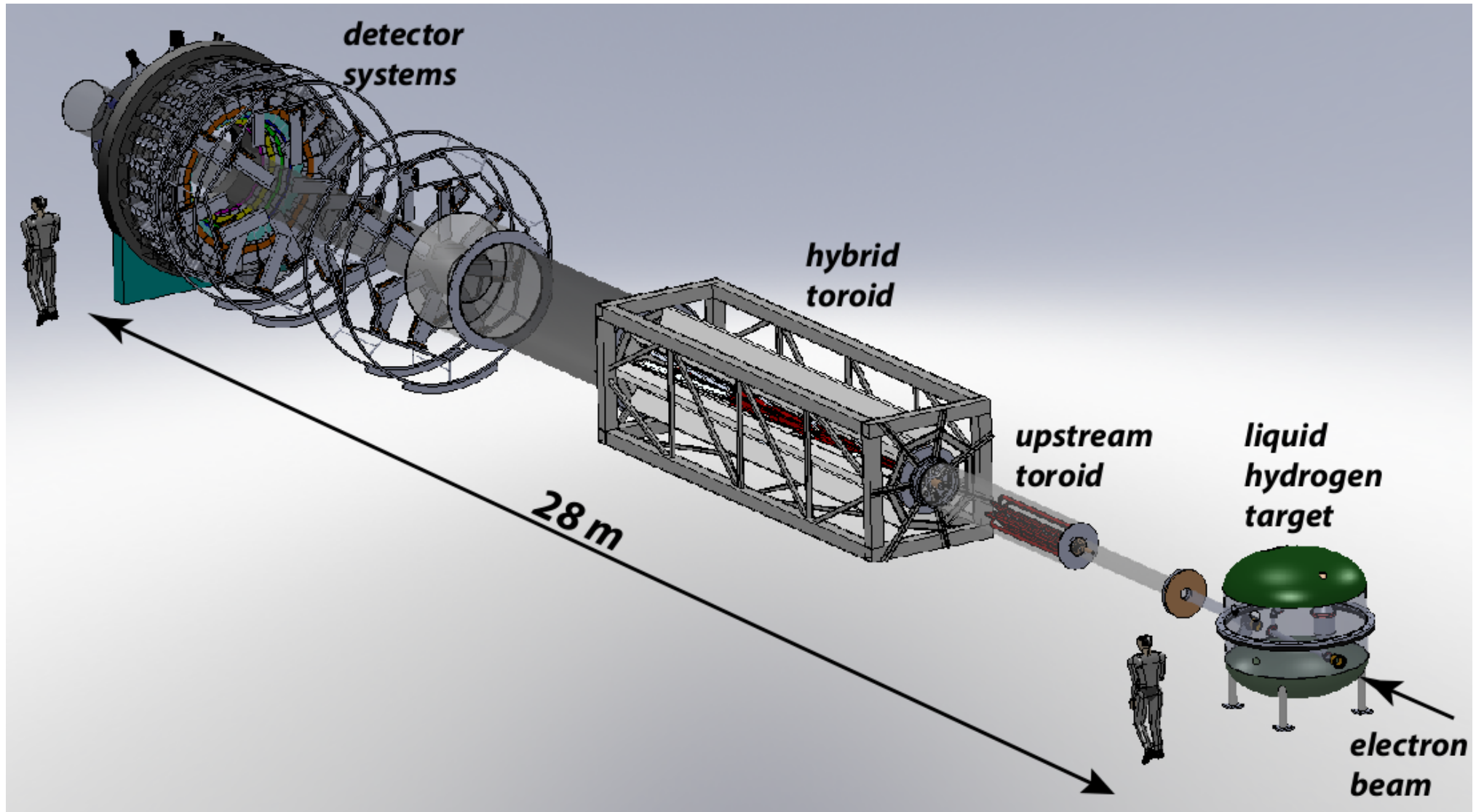
❖ Probe potential kinetic-mixing of super-light (10 to 500 MeV) dark Z bosons with SM Z

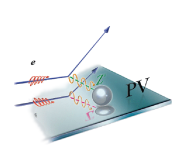




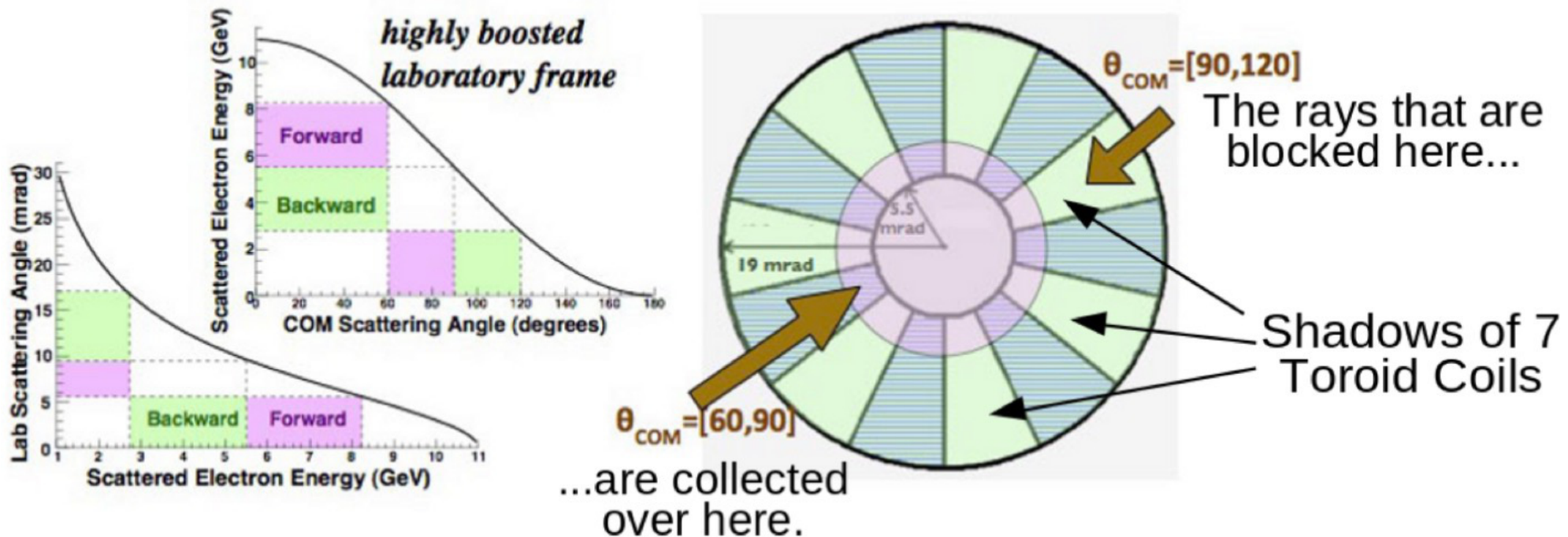
MOLLER Apparatus

(major new installation experiment for Hall A)

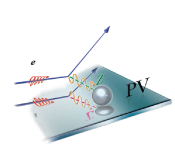




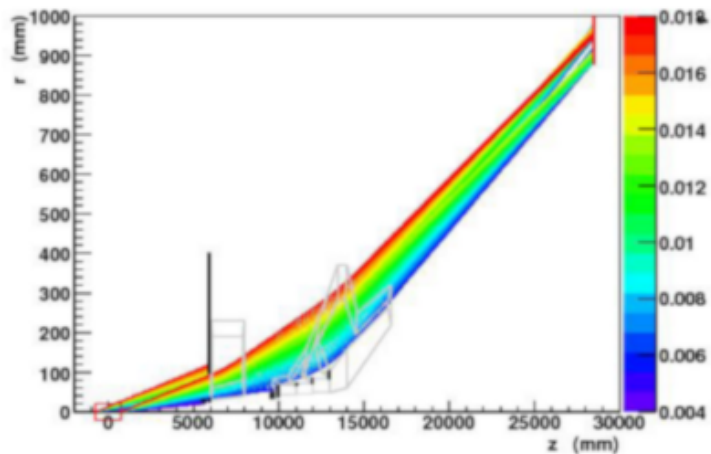
Optimized Spectrometer ($\sim 100\%$ Acceptance)



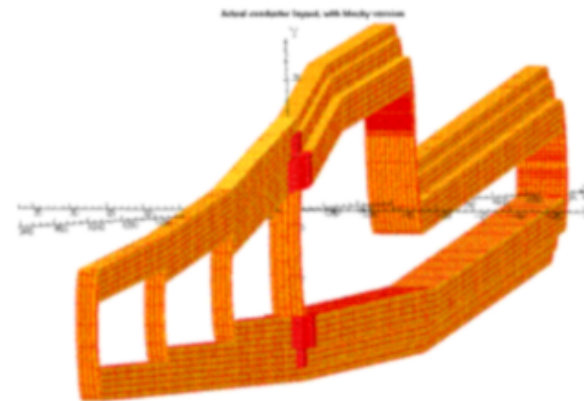
- The combination of a toroidal magnetic system with an odd number of coils together with the symmetric, identical particle scattering nature of the Møller process allows for $\sim 100\%$ azimuthal acceptance



Toroid Design Concept

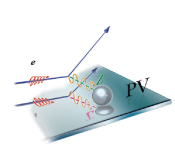


Projected radial coordinate of scattered Møller electron trajectories. Colors represent θ_{lab} (rad). Magnet coils (grey) and collimators (black) are overlaid.



Single Hybrid coil shown with 1/10 scale in z direction. Note the 4 current returns give successively higher downstream fields.

- Spectrometer employs two back-to-back toroid magnets and precision collimation:
 - Upstream toroid has conventional geometry
 - Downstream “hybrid” toroid novel design inspired by the need to focus Møller electrons with a wide momentum range while separating them from e-p (Mott) scattering background



MOLLER Integrating Detector Layout and Rates

- Spectrometer separates signal from bkgd and radially focuses at detector plane
- Rates for 11 GeV/75 μ A (80% pol.) beam, 1.5m liquid hydrogen target. See fig. \rightarrow
- Six radial rings, 28 phi segments per ring*
- Ring 5 intercepts Moller peak (\sim 150 GHz), Ring 2 intercepts bkgd "ep" peaks
- 250 quartz tiles: allow full characterization and deconvolution of bkgd and signal processes

